Progress in Biomedical Engineering

TOPICAL REVIEW • OPEN ACCESS

Optical spectroscopy for *in vivo* medical diagnosis—a review of the state of the art and future perspectives

To cite this article: Jang Ah Kim *et al* 2020 *Prog. Biomed. Eng.* **2** 042001

View the article online for updates and enhancements.

You may also like

- GRAVITATIONAL LENS MODELS BASED ON SUBMILLIMETER ARRAY IMAGING OF *HERSCHEL*-SELECTED STRONGLY LENSED SUB-MILLIMETER GALAXIES AT $z > 1.5$
R. S. Bussmann, I. Pérez-Fournon, S. Amber et al.

- THE CHANDRA MULTI-WAVELENGTH PROJECT: OPTICAL SPECTROSCOPY AND THE BROADBAND SPECTRAL ENERGY DISTRIBUTIONS OF X-RAY-SELECTED AGNs
Markos Trichas, Paul J. Green, John D. Silverman et al.

- The study of oxygenation dynamics during experimental tumor growth using frequency-domain diffuse optical spectroscopy
Tatiana Kalganova, Anna Maslennikova, Anna Orlova et al.

This content was downloaded from IP address 155.198.108.41 on 18/03/2024 at 20:15

IOP Publishing Prog. Biomed. Eng. 2 (2020) 042001 https://doi.org/10.1088/2516-1091/abaaa3

Progress in Biomedical Engineering



OPEN ACCESS

RECEIVED
20 February 2020

REVISED
21 June 2020

ACCEPTED FOR PUBLICATION
29 July 2020

PUBLISHED
26 August 2020

Original content from this work may be used under the terms of the Creative Commons Attribution 4.0 licence.

Any further distribution of this work must maintain attribution to the author(s) and the title of the work, journal citation and DOI.



TOPICAL REVIEW

Optical spectroscopy for *in vivo* medical diagnosis—a review of the state of the art and future perspectives

Jang Ah Kim[1,3], **Dominic J Wales**[1,3] and **Guang-Zhong Yang**[1,2]

[1] The Hamlyn Centre for Robotic Surgery, Imperial College London, London, SW7 2AZ, United Kingdom
[2] Institute of Medical Robotics, Shanghai Jiao Tong University, Shanghai 200240, People's Republic of China
[3] These authors contributed equally.

E-mail: j.a.kim@imperial.ac.uk **and** gzyang@sjtu.edu.cn

Keywords: optical diagnosis, spectroscopy, fluorescence, Raman scattering, elastic optical scattering

Abstract

When light is incident to a biological tissue surface, combinations of optical processes occur, such as reflection, absorption, elastic and non-elastic scattering, and fluorescence. Analysis of these light interactions with the tissue provides insight into the metabolic and pathological state of the tissue. Furthermore, *in vivo* diagnosis of diseases using optical spectroscopy enables *in situ* rapid clinical decisions without invasive biopsies. For *in vivo* scenarios, incident light can be delivered in a highly localized manner to tissue via optical fibers, which are placed within the working channels of minimally invasive clinical tools, such as endoscopes. There has been extensive development in the accuracy and specificity of these optical spectroscopy techniques since the earliest *in vivo* examples were published in the academic literature in the early '90s, and there are now commercially available systems that have undergone medical and clinical trials. In this review, several types of optical spectroscopy techniques (elastic optical scattering spectroscopy, fluorescence spectroscopy, Raman spectroscopy, and multimodal spectroscopy) for the diagnosis and monitoring of diseases states of tissue in an *in vivo* setting are introduced and explored. Examples of the latest and most impactful works for each technique are then critically reviewed. Finally, current challenges and unmet clinical needs are discussed, followed by future opportunities, such as point-based spectroscopies for robot-guided surgical interventions.

1. Introduction

Tissue-based diagnosis in medicine is the determination of the disease state of tissue/s within the body [1]. Its use during image-guided interventional procedures, such as endoscopy, bronchoscopy or laparoscopy can be achieved with observation by a trained clinician, although confirmation of diseases states may necessitate biopsy of the suspect tissue. However, the turnaround time of subsequent histopathological analysis of the biopsy sample, especially if on the order of days to weeks, can cause delays and complications, contributing to increased morbidity and mortality rates [2]. An alternative technique is point-based optical diagnosis. These point-based optical diagnosis techniques are used to measure optical characteristics of tissues *in vivo*. Because the optical properties of healthy and diseased tissues differ, this enables determination of the disease state of the tissue. Therefore, faster analysis and diagnosis of the disease state of the tissue leads to a higher rate of positive diagnosis and improved patient outcomes due to faster administering of the required treatment. Furthermore, this approach significantly reduces the trauma to the surrounding tissues as no invasive tissue biopsy is required. In addition, it is estimated that optical diagnosis will also increase surveillance intervals and thus reduce associated costs [3].

Consequently, point-based optical diagnosis techniques have enjoyed considerable research and commercial attention. There have been significant advances in the accuracy and specificity of these techniques since the earliest *in vivo* examples were published in the academic literature in the early '90s, and now there are commercially available systems that have undergone medical and clinical trials. However, optical diagnosis techniques have not fully replaced traditional biopsy techniques due to high cost and the

© 2020 The Author(s). Published by IOP Publishing Ltd

requirement for expert practitioners. Despite this, the future of point-based optical diagnosis systems is bright as the combination of multiple different techniques could revolutionalize the current clinical diagnosis paradigm. In addition, optical diagnosis techniques will allow for the advancement of robot-guided interventions.

Herein this review, a physical background to optical diagnosis techniques will be given, the state of the art will be critically assessed and future perspectives and opportunities will be highlighted to enable further advancements in this continually growing field.

2. Scope of the review

This review will cover deep, *in vivo* and quasi-real-time point-based spectroscopy, otherwise referred to as 'optical diagnosis'. In this review, the term 'deep' is defined as placement of the optical probe assembly inside the body either via a natural lumen or a surgical incision/opening. The term '*in vivo*' in this review refers to optical measurements of biological tissue (excluding blood) performed on either animal (developmental work) or human subjects that were not performed '*ex vivo*' or '*in vitro*'. In addition, we have only included animal studies where the animal was alive during the measurements. The term quasi-real-time is defined as optical measurements on a timeframe (ca. microseconds to minutes) that allows for a clinician or surgeon to make a medical decision during a medical operation or procedure. Finally, point-based spectroscopy is defined as a spectroscopic optical measurement performed at an individual site on/in biological tissue during the acquisition of the spectrum or spectra, and is not a wide-area imaging or raster-scanning based measurement. A 'site' is defined by the dimensions of the probe (if the probe is in direct contact with the tissue) or illumination spot, which is typically a few tens or hundreds of micrometers in diameter. This approach is in contrast to imaging techniques, which typically illuminate and collect light from much larger areas, ca. millimeters to centimeters. Therefore, this review does not cover endoscopic imaging measurements of tissues, but for the interested readers, there are many excellent reviews [4–8]. To achieve medical diagnosis using optical spectroscopic data, data processing techniques and diagnostic algorithms are crucial. Substantial research on the development of algorithms is ongoing. The focus of this review is mostly centered on the hardware of the optical diagnosis systems, since the aim of this review is to introduce the fundamentals of light-tissue interactions and the latest clinical examples of *in vivo* optical diagnosis technologies. Further brief discussion about diagnostic algorithms based on machine learning techniques is given in section 6. **Current status and future perspectives**, but for a more complete overview we point interested readers to the literature [9–13]. Finally, this review focuses on the most recent examples of *in vivo* use optical diagnosis techniques, or on the techniques with the highest technical readiness levels. However, it should be noted that in each section there is a thorough list of references describing previous works for each technique.

3. Theoretical and technical background of real-time *in vivo* optical diagnosis

When light is incident to a tissue surface, it can result in a combination of various optical processes, such as reflection, absorption, scattering, and fluorescence (figure 1(A)). Spectroscopic analysis of each of these optical processes provides various information of the optical properties of tissues that can be diagnostically meaningful. Among the wide range of available techniques, elastic scattering spectroscopy, fluorescence spectroscopy, and Raman spectroscopy are the techniques that have been most intensively developed and implemented for point-based, real-time *in vivo* optical diagnosis deep inside the body, and therefore, these three spectroscopic techniques are discussed in this review. Generally, each spectroscopic technique is applicable to different diagnostic factors of interest. Elastic optical scattering spectroscopies (EOSS) are used to measure cellular/subcellular morphology of the epithelial layer. Diseased tissues (e.g. inflamed tissues and tumor tissues) exhibit abnormal cellular/subcellular morphologies, such as loosening of epithelial barrier, enlarged nucleus, cell crowding and disorganization, etc [14], which induce differences in the EOSS spectra between normal and diseased tissues (figure 1(B) **Elastic optical scattering**). Fluorescence spectroscopies (FS) provide the state of cell metabolism. Metabolic pathways are disrupted in diseased cells, and thus the redox balance and the concentration of metabolites change as disease progresses. For example, the metabolic activity of cancerous cells is enhanced as tumors develop, resulting in increased production of NADPH (the reduced form of nicotinamide adenine dinucleotide phosphate) and metabolites (e.g. lactate) [15]. Changes in concentration of these cofactors (NADPH) and metabolites upon disease progression can be characterized with FS using either intrinsically fluorescent endogeneous fluorophores or tagged with exogenous fluorophores (figure 1(B) **Fluorescence**). Finally, Raman spectroscopies (RS) are used to interrogate the molecular signature of the tissue. All the aforementioned pathological features of diseased tissues and cells also play a role in diagnosis using RS. More specifically, RS provides information on chemical composition and structure of target analytes. Since fundamentally most biomolecules are Raman active, changes in the

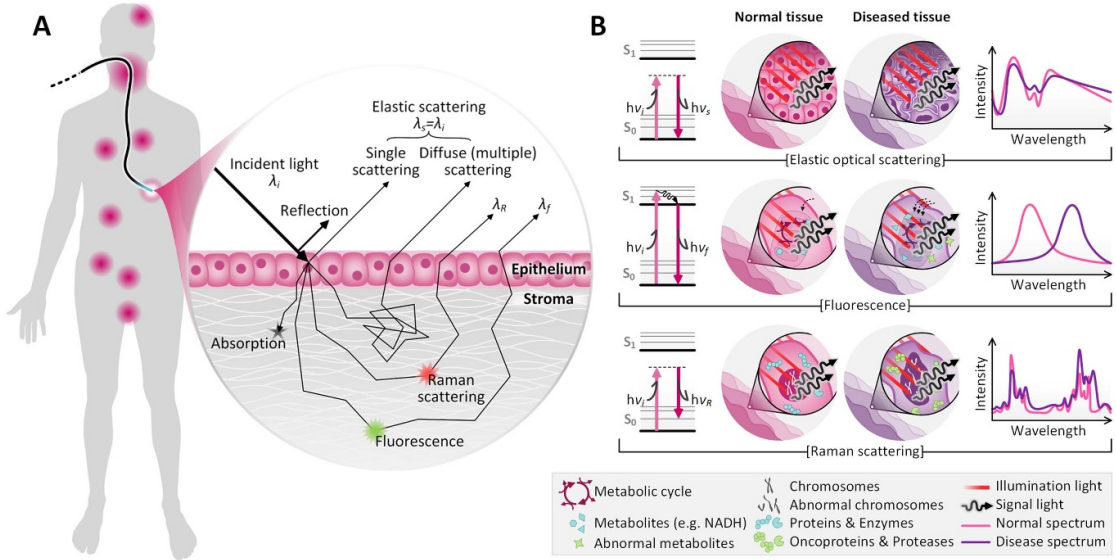


Figure 1. Target locations of point-based *in vivo* optical diagnosis, types of light-tissue interactions and spectroscopic diagnosis mechanisms of elastic optical scattering, fluorescence, and Raman scattering. (A) Point-based *in vivo* diagnosis can be utilized where current minimally invasive surgery/intervention, flexible endoscopy, and natural orifice transluminal endoscopic surgery can access, e.g. upper/lower gastrointestinal tract, artery, heart, bladder, cervix, etc (left). Several optical processes occur at the uppermost layers of tissues (from epithelial layer to stromal layer) as a result of light-tissue interaction; surface specular reflection, absorption, elastic optical scattering, fluorescence, and Raman scattering (right). λ_i, λ_s, λ_f, and λ_R are wavelengths of incident light, elastically scattered light, fluorescence, and Raman scattering, respectively. (B) Representative illustrations of Jablonski diagrams for each spectroscopic technique, where S_0, S_1, h, and ν represent the ground energy level, the excited energy level, Planck's constant, and frequency of light (left), respectively. The dotted lines in the Jablonski diagrams for elastic scattering and Raman scattering represent virtual energy levels. Spectroscopic techniques based on elastic optical scattering, fluorescence, and Raman scattering are capable of disease diagnosis by characterizing cellular/subcellular structures, cell metabolism states, and molecular signatures of normal and diseased tissues, respectively (middle). Illustrative examples of the differences in spectroscopic features between normal and diseased tissues (right).

concentration, deformation and mutation, and production of new compounds due to disease can exhibit distinctive RS signals (figure 1(B) **Raman scattering**). Indeed, in cancer progression, quantities and/or conformation of nucleic acids, proteins, lipids, and carbohydrates change [16]. In this section, the introductory overview of these three main spectroscopic techniques used for optical diagnosis is addressed.

3.1. Elastic optical scattering spectroscopy (EOSS)

3.1.1. Physical background

Light scatters when encountering any spatial inhomogeneity in refractive index. Micro and nanoscale particles in gas or liquid media are the simplest scattering models and, in most cases, the process does not entail changes in photon energy ($h\nu_s = h\nu_i$, so called 'elastic' as shown in figure 1(B) **Elastic optical scattering**, cf Raman scattering as an 'inelastic' scattering process that entails energy loss or gain. Details in section 3.2). Scattering in tissue is significantly more complex due to the high sub-microscopic complexity of tissues, which is interlinked with local refractive index variation. Indeed, the refractive index of tissue (n) can be defined as $n = n_0 + \alpha\rho$, where n_0 is the refractive index of the liquid medium (i.e. water), α is the proportionality coefficient, and ρ is the portion of tissue solids (e.g. proteins, lipids, DNA, etc) by volume, all of which significantly vary in different tissue types and are difficult to quantify precisely. Overall, size, shape, refractive index, size distribution, and number density of cellular/subcellular structures determine spectral features of the scattered light. Measurement of light scattering in tissue can therefore be particularly useful for diagnosis of disease states that accompany changes in cellular/subcellular morphology and spatial distribution—i.e. neoplastic development of epithelia from dysplasia to invasive cancer (despite a dependence on types of epithelia and types of cancer).

In tissue optics, key parameters that characterize the light scattering are the scattering cross sections, σ_s (describing the total scattering power of a scattering object), the scattering coefficient, μ_s (the probability of a photon to be scattered), the anisotropy coefficient, g (the tendency to be scattered forwardly, i.e. forward scattering $g = 1$, isotropic scattering $g = 0$, backscattering $g = -1$), and the reduced scattering coefficient, $\mu'_s = \mu_s(1 - g)$. These parameters can be derived from the scattering matrix, **S**, which formally should be obtained by solving Maxwell's equations. However, solving Maxwell's equations for scattering in tissue is very difficult due to the sub-microscopic complexity as mentioned above. Therefore, use of approximations or numerical methods to calculate the scattering matrix is unavoidable. Although there are several

approximations available to calculate the scattering matrix, such as the Rayleigh scattering model, the Rayleigh-Gans-Debye (RGD) approximation, the Van de Hulst approximation, etc, none of these approaches alone can precisely describe scattering events by cellular/subcellular structures in tissue because each approach is only valid for limited ranges of scatterer size and the relative refractive index. For example, the Rayleigh scattering model is valid when the scatterer is very small, $ka \ll 1$ where $k = 2\pi\,\lambda^{-1}$ is the wavenumber of the light, λ is wavelength of the light, a is the scatterer's radius, which cannot apply to subcellular organelles greater than 50 nm in visible range (i.e. nucleus—5–10 μm, mitochondria—1–2 μm in the long axis and 0.2–0.8 μm in the short axis, lysosomes—250–800 nm, peroxisomes—200–1000 nm). RGD approximation, on the other hand, is valid when $ka|n' - 1| > 1$ where $n' = n_{\text{organelle}}/n_{\text{cytoplasm}}$ is the relative refractive index. Considering that the refractive index of most subcellular organelles ranges from 1.38 to 1.42 and that of the cytoplasm is within 1.34 to 1.36 (thus $n' - 1 \approx 0.01$–0.05), the RGD approximation works well for describing scattering events by the majority of subcellular organelles except the nucleus [17]. However, it is not sufficient to describe forward scattering that is dominant in scattering events by larger scatterers (i.e. nuclei). The Van de Hulst approximation can describe forward scattering by larger scatterers when two conditions are met: $ka|n' - 1| > 1$ and $|n' - 1| \ll 1$. Nevertheless, backscattering can be easily neglected by this approach. Approximation of the nucleus as a spherical scatterer, however, enables the exact solution by the Mie theory. Although the Mie theory is valid for isolated homogeneous spheres, which does not represent tissue sub-microscopic structures, it has been widely accepted for describing scattering in tissue. This is partly due to a lack of better alternatives, but, more importantly, because it is still able to provide an important physical picture of scattering from subcellular organelles of any size. Since the Mie theory is an exact solution of Maxwell's equations, numerical methods, such as finite-difference time-domain (FDTD) calculations, T-matrix, discrete dipole approximation (DDA), etc, are required. Lists of scattering properties (e.g. μ_s, g, μ'_s, n) of different tissues reported, and details of the approximation approaches are available in ref [18] and ref [19], respectively.

3.1.2. Technical background

In vivo spectroscopy in general needs three fundamental elements—a light source, a detector, and a fiber-optic probe that guides source light to analytes and collects and guides back the signal light to the detector. Selection of appropriate light source, detector, and probe design is essential to facilitate reliable measurement. Additional optics, such as lenses, filters, polarizers, and beam splitters may also be required for further treatment of the source/signal light. For EOSS, broadband light sources are used since the scattering parameters listed in the previous section are functions of wavelength. Xenon lamps, nearly uniformly emitting from ultraviolet (UV) to near infrared (NIR) range (320 to 900 nm), are generally preferred for EOSS as shown in figure 2. Other white light sources (e.g. white light LED), of which wavelengths are within visible range from 500 nm to 700 nm, also perform well for EOSS. This point, along with the fact that EOSS does not typically require extra optics for light source and detector, permits the measurement system to be inexpensive and simple. However, absorption by chromophores (e.g. hemoglobin, water, fat, melanin, etc) interferes the EOSS measurement by adding extra complexity to the resulting spectra in this wavelength range. Soret band (400 to 440 nm) and Q band (540 to 580 nm) are the most prevalent and intense absorption features by hemoglobin and its oxygen saturation levels. Although absorption by water molecules is negligible within the working wavelength range below 900 nm, absorption coefficient of fatty tissues and melanin may induce unwanted spectral features to the EOSS spectra. Since elimination of the absorption effect by these existing chromophores, especially in an *in vivo* environment, is often impossible, an empirically modeled absorption coefficient of tissue should be taken into account in order to extract a useful EOSS signal containing information about cellular/subcellular structures of tissues. Monte Carlo simulation has often been performed prior to practical trials to estimate contributions of both absorption and scattering.

Specular reflection at the probe-tissue contact and diffuse reflection resulting from multiple scattering are another concurrent event to be dealt with when measuring backscattered light from a tissue. These events also add extra background spectral features to the EOSS spectra, leading to difficulties in extraction of meaningful signal associated with cellular/subcellular structures of tissues. Fortunately, these effects can be minimized by effective probe designs with appropriate geometries. Bevelled tip-probes [20–22] have been useful for minimizing reception of specular reflection at the probe-tissue contact through collection fibers.

Diffuse reflection spectra (DRS) resulting from multiple scattering can be excluded by reducing separation distance between illumination fiber and collection fiber. Through multiple scattering, the scattering trajectory is randomized and gets longer (thus reaching laterally far from the illumination fiber) until when the result scattering signal is collected. Despite varying in different tissue types, this multiple scattering trajectory can be ranging from a few-hundred-microns to a few millimeters laterally. Therefore, designing the correct illumination-to-collection fiber separation (S_{ic}) is important to avoid collecting the multiple scattering signal. In the working wavelength range from visible to NIR, a rough boundary above

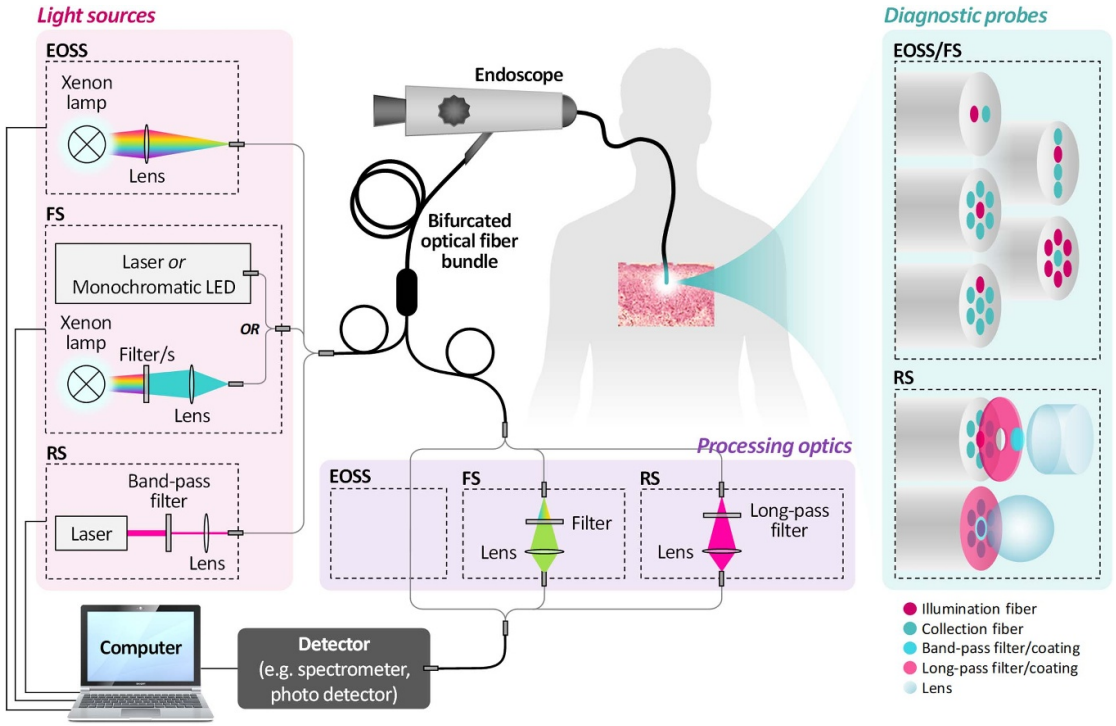


Figure 2. A comprehensive schematic of implementation settings of the point-based *in vivo* optical diagnostic techniques; elastic optical scattering spectroscopy (EOSS), fluorescence spectroscopy (FS), and Raman spectroscopy (RS). *In vivo* spectroscopy in general needs three fundamental elements—a light source, a detector, and an optical fiber probe that guides source light to the tissue and collects and guides back the signal light to the detector. Xenon lamp can be replaced by other broad-band (white) light sources. Spectrometers are not always preferred, e.g. simple photo detectors can be used for cost-effective and faster FS. Extra optics for effective light coupling and filtering are sometimes required in front of light sources and detectors (see boxes 'Light sources' and 'Processing optics'). Typical diagnostic probes contain at least one illumination fiber and one collection fiber, allowing diverse fiber arrangements (see EOSS/FS section in box 'Diagnostic probes'). Multiple number of illumination fibers and collection fibers are used in order to improve signal collection efficiency (1 illumination fiber/6 collection fiber and 6 illumination fibers/1 collection fiber, the latter is adapted with permission from [23] © The Optical Society). These fibers can be arranged linearly (1 illumination fiber/3 collection fibers), adapted with permission from [21] © The Optical Society, or off-centered (1 illumination fiber/6 collection fibers), Copyright © 2017, Springer Nature. For RS probes, additional filters and lenses at the distal end are also favorable to maximize the performance (see RS section in box 'Diagnostic probes'). The probe schematic with a rod lens is from [254]. Reprinted with permission from AAAS. The probe schematic with a ball lens is adapted with permission from [261] © The Optical Society.

which multiple scattering events occur can be designated as $S_{ic} \approx 350\ \mu$m (i.e. multiple scattering signal is collected by a probe with $S_{ic} \geq 350\ \mu$m).

An EOSS probe includes at least an illumination optical fiber and a collection optical fiber. Numbers, diameters, and arrangement of illumination/collection optical fibers may vary depending on applications. Probe designs with several illumination fibers surrounding a single collection fiber that allow improved signal collection efficiency have been reported (6 illumination fibers/1 collection fiber [23], 7 illumination fibers/1 collection fiber [24]). There has been a greater variety of probe designs having a single illumination fiber but multiple collection fibers (e.g. 1 illumination fiber/2 collection fibers to 10 collection fibers). These fibers are not always arranged to be axially asymmetric but often linear [21, 25–29] or having an off-centered illumination fiber [30–32] in order to incorporate various S_{ic} values (thus the scattering angle) within a probe (see EOSS/FS section in box 'Diagnostic probes' in figure 2). These probe configurations allow collecting both EOSS signal from the uppermost epithelial layer and multiple scattering signal from the deeper tissue as a background to ultimately enable reliable extraction of EOSS signal from the diffuse reflection signal.

3.2. Fluorescence spectroscopy (FS)

3.2.1. Physical background

Fluorescence is defined as 'spontaneous emission of radiation (luminescence) from an excited molecular entity with retention of spin multiplicity' [33]. A brief overview of the physics of fluorescence will be discussed here. A detailed explanation of fluorescence is out of the scope of this review, but for the interested reader a more in depth overview is available here [34–36].

Upon absorption of a photon of the appropriate wavelength in the UV-visible region, an electron within the ground state (S_0) of a molecule can be elevated to a higher vibrational state of an excited molecular

singlet state (S_1), with the electron retaining the same spin as in the ground state. This process occurs in ca. 10^{-15} s. Then the excited electron most commonly undergoes internal conversion, wherein the electron relaxes to the lowest vibrational level of S_1 and this process occurs in ca. 10^{-12} s. After internal conversion, the electron can return to the S_0 either radiatively or non-radiatively, depending on the available de-excitation pathways. The possible non-radiative pathways include quenching, fluorescence resonance energy transfer (FRET) and other non-radiative decay mechanisms. The radiative pathway is fluorescence. During the radiative pathway decay to the ground state, the electron releases the excess energy as an emitted photon (ca. 10^{-8} s, figure 1(B) **Fluorescence**). In the ideal case, there is a single S_1 and a single S_0, thus the mean time between absorption of a photon and emission of the fluorescence photon is designated as the fluorescence lifetime, τ. Measurements of absorption and fluorescence (both intensity and lifetimes) of biological tissues allows for monitoring of changes in electronic energy states of the molecules that comprise the tissue and thus provides biochemical information for diagnostics.

All biological tissue exhibits endogenous fluorescence, known as autofluorescence, when irradiated with light of the appropriate wavelength. This is because biological tissues contain many endogenous fluorophores such as; NADH (the reduced form of nicotinamide adenine dinucleotide), NADPH, flavins, collagen, elastin, tryptophan, retinol and porphyrins, amongst others [37]. Furthermore, each fluorophore has specific and characteristic excitation and emission spectra.

The concentration of endogenous fluorophores within biological tissue can change due to metabolic changes caused by a range of pathological processes, such as inflammation and dysplasia [37]. Therefore, in an ideal case, a quantitative measurement of the fluorescent intensity of the autofluorescence spectrum of tissue, or a particular fluorophore, can reveal the pathological state of the biological tissue. However, in reality, the situation is more complex, as different fluorophores fluoresce at different intensities, different wavelengths of excitation light penetrate to different depths into the tissue before complete absorption, and also wavelength dependent scattering or reabsorption occurs as biological tissues are turbid media [38, 39]. Furthermore, the excitation and emission spectra of multiple fluorophores can overlap and thus an undesirable 'background fluorescence' signal can further complicate the deconvolution of tissue fluorescence spectra for determination of the concentration of the desired tissue components.

Therefore, several correction strategies have been proposed including the use of the ratio of fluorescence intensity to reflectance intensity [40], a ratio of fluorescence intensities at two different emission wavelengths [41] and also more complex correction models based on Kubelka-Munk theory [38]. However, each of these correction strategies has intrinsic advantages and disadvantages and indeed, work continues to develop faster and/or more precise correction strategies [42]. To overcome the problems of 'background fluorescence' there are two main solutions. The first is the use of exogenous fluorophores. An exogenous fluorophore is an externally administered fluorophore that can be chosen to have a particularly intense fluorescence emission and thus this fluorescence emission can be clearly measured above the background. An additional benefit of exogenous fluorophores is that they can pre-concentrate in neoplastic tissues and thus further improve the discrimination of 'abnormal' tissue from 'normal' tissue. The second solution is the use of wavelength and band-pass filters to remove the rest of the background fluorescence and this is further discussed in the technical background sub-section below.

3.2.2. Technical background

Here a brief overview of the technical aspects of point-based fluorescence spectroscopy for tissue measurements will be discussed. For the interested reader a more in depth overview is available here [43].

Typically a light-induced fluorescence spectroscopy (LIFS) system is used to perform point fluorescence spectroscopy (as opposed to fluorescence endoscopy imaging [5]). A LIFS system (figure 2, see FS sections) consists of either a broadband white light source or a monochromatic light source (e.g. continuous-wave or pulsed lasers, LEDs) coupled into a small-diameter probe, which may consist of either one or a bundle of optical fibers. In the case of a bundle of optical fibers, some of the fibers deliver the excitation light whilst the surrounding fibers collect the fluorescence emitted light (figure 2, EOSS/FS section in box 'Diagnostic probes'). The probe can be placed within the instrument channel of an endoscope or used independently. During a measurement, the probe is placed in intimate contact with the tissue for a specific and sufficient amount of time for the particular measurement, allowing for the emitted fluorescence light to be transmitted back to the detector via optical filters that filter out the background fluorescence. Commonly, LIFS systems are used without administering exogenous fluorophores, but the use of exogenous fluorophores combined with use of a point-based LIFS system has also been reported [44–48]. More recently, LIFS systems have evolved with time and wavelength resolved systems demonstrated. A driving force for the evolution of the technique is the difficulty to conduct absolute emission intensity measurements *in vivo* because measurements are affected by multiple factors. These factors include physical factors such as tissue movement and surface profile, which may cause a change in light excitation-collection geometry and

non-uniform illumination, respectively. The confounding photochemical factors are photobleaching and the presence of, and variation in concentration of, endogenous absorbers.

One way to overcome these challenges is by using the alternative method of time-resolved fluorescence spectroscopy, in which fluorescence excited state decay lifetimes are also measured as an orthogonal variable. Time-resolved fluorescence spectroscopy affords several advantages. Firstly, fluorescence lifetimes are independent of fluorescence intensities, which can be affected by non-uniform illumination and tissue movement. Additionally, biomolecules and tissues will have unique fluorescence decay lifetimes and thus this allows for spectral resolution of biomolecules that may have overlapping fluorescence emission spectra. Fluorescence decay lifetimes are also affected by local changes in the local physiochemical and metabolic environments of the tissue, due to the effect that the local tissue microenvironment has on quenching rates of biomolecules. Therefore, further biochemical information from the tissue of interest can be gathered. An excellent in-depth review on time-resolved fluorescence spectroscopy is provided by Marcu [49].

3.3. Raman spectroscopy (RS)

3.3.1. Physical background

Raman scattering is an inelastic scattering process of a photon that either loses or gains a certain amount of energy as a result of light–matter interaction. The amount of energy difference expressed by the emitted photon during the Raman scattering process corresponds to specific vibrational modes of chemical bonds in a molecule (an example of energy loss process, i.e. Stokes Raman scattering, figure 1(B) **Raman scattering**). The energy difference appears as a shift in the spectrum (so called 'Raman shift') and the technique that analyses molecular information of substances (i.e. molecular structure, chemical bonding, functional groups, interaction between molecules and the surrounding environment, and physical state) by measuring the Raman shift is Raman spectroscopy (RS). It was first experimentally observed by Chandrasekhara Venkata Raman in 1928 [50]. Since then, Raman spectroscopy has become an essential analytical tool that is vital in various applications, such as pharmaceutics [51], forensic science [52–54], mineralogy [55], carbon materials [56–58], semiconductors [59], and life science [12, 60–62]. This is due to its advantages of high molecular specificity, high resolution, non-destructive and non-contacting measurement, and flexibility in sample forms and volumes. In particular, RS facilitates detection of aqueous samples without any interference of water signals due to insensitivity to molecules with large dipoles, and consequently RS is used in biomedical applications [62].

RS of biological samples (e.g. tissues and biofluids), therefore, enables detection of characteristic spectral features indicating the pathological state of the samples. Various vibrating modes of chemical bonds in the backbones and side-chains of lipids, proteins (complicated combination of motions from different parts of amino acid backbone and secondary structure), and nucleic acids (from O–P–O backbone and individual nucleotide bases) participate in the Raman spectra of biological samples [62]. These features are generally observed in the 'fingerprint regio*n*' which is from 600 to 1800 cm^{-1} in a very complex superimposed manner with multiple sharp peaks. Most of the spectral analysis is done within this range for biological samples. Some features may also be found in much higher energy range above 2500 cm^{-1} up to 3400 cm^{-1} (so called the 'high wavenumber regio*n*') mostly indicating independently vibrating hydrogen atoms. RS of biological samples is sensitive to changes in the chemical compositions of these molecules (lipids, proteins, and nucleic acids), which can be ascribed to disease states, and thus allows for accurate molecular diagnosis of diseases.

Detailed vibrational modes and corresponding wavenumbers of chemical bonds and structures found in biological molecules are presented elsewhere [60, 62, 63].

3.3.2. Technical background

Despite the exclusive advantages of RS, it is often referred as an insensitive technique because it is an inherently weak process occurring approximately once in hundred million compared to elastic (Rayleigh) scattering [61]. Advancement in high power laser sources and precision optics in the past decades has allowed reliable performance of RS. Essentially, a band-pass filter (or a laser line filter) is used for refining the excitation laser quality to be sharp and monochrome and a long-pass/notch filter is required to reject the Rayleigh scattering (figure 2, see RS sections in boxes 'Light sources' and 'Processing optics'). Nevertheless, better sensitivity and signal-to-noise level are still required especially for practical applications than laboratory-based situations. To this end, diverse enhancement techniques have been proposed and developed, for instance, coherent anti-Stokes Raman scattering (CARS), stimulated Raman scattering (SRS), surface-enhanced Raman scattering (SERS), tip-enhanced Raman spectroscopy (TERS) and more [64, 65].

Moreover, *in vivo* RS particularly requires additional attention to the control of background signal. Auto-fluorescence of tissue may also interfere with the Raman spectrum and degrade the signal-to-noise ratio. Contribution of autofluorescence can be rejected by selecting the appropriate light-source with the appropriate excitation wavelength. Because autofluorescence of most common biological tissues appears

under visible range excitation shorter than 700 nm, NIR light allows for minimized fluorescence in biological tissues. Typically, 785 nm, 830 nm, and 1064 nm NIR lasers are used for RS, although 1064 nm is not suitable for *in vivo* application because intensity of the radiation drastically drops with the fourth power of incident wavelength, which results in a poor signal collection efficiency [62]. Other than control of materials and components, further technical approaches to reject extra fluorescence have also been achieved in diverse ways, e.g. modulated Raman spectroscopy (MRS) [66], time-gated RS [67], and Fourier transform RS [68]. In addition to the autofluorescence of tissues, silica—a typical material for optical fibers—exhibits a very strong photoluminescence background appearing as broad humps in Raman spectra. It easily overwhelms narrow and relatively weak Raman peaks, unless rejected, resulting in deterioration of the signal quality. To minimize this, various approaches have been proposed. For instance, integration of filtering and beam steering optics at the distal end of the probes [69–76] (figure 2, see RS section in box 'Diagnostic probes') and using other types of fibers such as hollow-core fiber [77], photonic crystal fiber (PCF), and double-clad fiber (DCF) [78] have been reported so far. Despite the huge effort, the fluorescence background cannot be completely removed and generally remains in the collected spectra. Post-processing of the collected signals is, therefore, always required to minimize both fluorescent artefacts in the final spectra. Polynomial fitting and subtraction of background are carried out regardless of configuration, with and without additional optics or different materials as mentioned above [79–82].

3.4. Multimodal spectroscopy

All of the techniques mentioned above have inherent advantages and disadvantages. Therefore, in an attempt to overcome the drawbacks of each individual technique, and to combine the advantages, there have been many examples of combining multiple spectroscopic techniques into one device. For example, FS generally has a high signal strength, but lacks specificity, whereas RS has a high degree of specificity and sensitivity to chemical/molecular changes in tissue, but has low signal strength. Therefore, a combination of the two orthogonal modalities allows for the mitigation of the drawbacks of both techniques and allows for more metabolic and pathological information to be gathered during the optical diagnosis [83].

Combined spectroscopy systems are referred to as multimodal spectroscopy devices and invariably the light is delivered to the tissue and collected from the tissue through the same probe assembly. Typically, FS is combined with one or more other techniques, such as FS combined with DRS (FS + DRS) or FS combined with both RS and DRS (FS + Raman + DRS).

4. Technology readiness levels (TRLs)

A technology readiness level (TRL) is a formal metric-based measurement of the maturity of hardware and/or software to be used in a system [84]. Therefore, in terms of clinical systems, such as optical diagnosis systems, TRLs can provide an overview metric on the progress of the system, from an initial concept or idea (TRL = 1) up to commercially validated and available (TRL = 9). Thus, in table 1, the highest TRLs for each optical diagnosis system defined in the sections above are given to provide an overview of the maturity of each technique, when applied to diagnosis within each organ system. We have determined the TRL levels of the spectroscopic techniques based on the definitions given by the US Department of Defense and Puppels *et al* [84, 85].

Typically, TRLs 1 & 2 are assigned to technologies that are at initial conceptual stages and these are not considered in this review. Here we have reviewed/meta-analyzed technologies that are at a level of maturity indicated by a TRL of $\geq$3. Therefore, we have grouped TRLs 3–9 into the following groups; Group A: TRLs 3–4, Group B: 5–7 and Group C: 8–9. Our particular sorting of the TRLs into these groups was guided by the TRL milestone groups as suggested by the US Department of Defense [86]. Thus, classification Group A contains technologies/systems that have been demonstrated in preliminary laboratory and/or animal model experiments, with some degree of analysis development, such as algorithms. Classification Group B contains technologies/systems that have been demonstrated and tested in clinical environments and trials, preferably in multiple-center trials. Finally, Group C contains technologies/systems that have been released to end-users commercially, with TRL = 9 representing a fully distributed and marketed product.

As can be seen in table 1, each technology has a different TRL when taking into account the different target organ systems that the technology has been used on. One of the main reasons for this is the challenge of accessibility of each probe design to each particular target organ system, when considering minimally invasive surgery (MIS) and intervention. For example, the optical diagnosis systems used for diagnostic measurements in the alimentary tract are generally the most mature. This is due to the easily accessible lumen (esophagus) and the plethora of available endoscopic devices designed for the alimentary tract, which can be easily adapted to contain optical diagnosis probes within the endoscope working channel.

Table 1. Spectroscopic techniques categorized by TRL classification groups (Group A: TRLs 3–4, Group B: 5–7 and Group C: 8–9)—a measure of the maturity of each technology.

Techniques	Target organ	TRL group
EOSS	Alimentary tract	B
	Brain	A
	Cervix	A
	Liver	B
	Lung	B
	Pancreas	B
FS	Alimentary tract	C
	Arteries & heart	C
	Bladder	B
	Brain	B
	Breast	B
	Cervix	C
	Endocrine	B
	Head & neck	B
	Liver	B
	Lungs	B
	Prostate	B
RS	Alimentary tract	B
	Artery	B
	Bladder	A
	Brain	B
	Breast	A
	Cervix	B
	Head & neck	B
	Lung	A
FS + Doppler Flowmetry	Brain	B
FS + DRS	Alimentary tract	B
	Arteries & heart	A
	Bladder	A
	Brain	B
	Cervix	C
	Head & neck	B
	Liver	B
FS + DRS + EOSS	Alimentary tract	B
	Cervix	B
	Head & neck	B
FS + RS + DRS	Alimentary tract	A
	Arteries & heart	A
	Brain	B
	Breast	A
	Head & neck	B
	Lung	A
FS + RS	Breast	A
	Head & neck	B

5. Clinical examples of spectroscopic sensing techniques

For brevity, only the most recent examples in the literature of the different optical diagnosis systems will be described. In addition, for each technique, the current state-of-the-art in terms of higher TRL groups will be discussed. However, it should be noted that for each technique there will be a comprehensive list of references of published deep and *in vivo* optical diagnosis measurements grouped by organ/disease types for the reader's interest, except for the multimodal spectroscopy section, wherein the references are grouped by spectroscopic technique.

5.1. Examples of EOSS

Examples of EOSS as a tool for diagnosis of disease by measuring different scattering coefficients of normal and abnormal tissues have been demonstrated for brain [87, 88], cervix [23, 30], gastrointestinal tracts [11, 28, 89–93], esophagus [94–96], head and neck (larynx, pharynx, oral cavity) [97], and pancreas [29, 32].

There are three representative EOSS probes that are considered as the most mature and have been demonstrated on patients (figure 3). One was initially developed by, and its diagnostic algorithm for *in vivo* colorectal cancer screening was demonstrated by, Bigio and colleagues, in 2011 (elastic scattering spectroscopy, ESS) [11, 91]. A dual fiber probe (outer diameter of 0.47 mm) comprised of an illumination fiber and a collection fiber, both having 200 μm core diameter, was integrated within a central lumen of conventional biopsy forceps. The center-to-center separation, or S_{ic}, between the fibers was 250 μm, which allows for ESS interrogation of 350 μm in depth which corresponds to a volume smaller than 0.2 mm^3. The jaws of the forceps were opened and the central optical probe was gently placed in contact with the tissue surface to take rapid ESS measurements when a polyp or suspicious growth was observed during the colonoscopy. Cooperative physical biopsy collection was also carried out by closing the jaws of the forceps once the optical readings were obtained. A compact table-top ESS system was also developed alongside with the probe. A clinical feasibility of this system was demonstrated for differentiation of neoplastic polyps from non-plastic polyps from 83 patients [32] (figure 3**. I.**). From the ESS measurement of 218 polyps (133 non-neoplastic and 85 neoplastic as histopathologically classified) a sensitivity of 91.5%, specificity of 92.2%, and accuracy of 91.9% with a high-confidence rate of 90.4% was achieved. Importantly, the group demonstrated that diminutive polyps that are smaller than 5 mm (n = 157) were successfully identified by ESS with a slightly lower sensitivity, specificity, and accuracy. These results were particularly promising because screening of neoplasia in polyps smaller than 5 mm directly relates to the American Society for Gastrointestinal Endoscopy (ASGE) Preservation and Incorporation of Valuable Endoscopic Innovations (PIVI) guidelines for the real-time endoscopic assessment for the histology of diminutive colorectal polyps.

The other probe was developed by Backman *et al* in 2012 [21]. The working principle of the low-coherence enhanced backscattering spectroscopy (LEBS) technique that they developed fundamentally shares the same physical background with EOSS, but includes extra features of the enhanced backscattering spectroscopy (EBS) technique. In particular, they took into account enhancement of the backscattered light around the exact backscattering direction, that is caused by the constructive interference of light waves propagating along a pair of time-reversal trajectories. This approach allowed EBS to be wavelength-sensitive and depth-selective so that it was effective for tissue diagnosis. The probe comprised of linear arrangement of four optical fibers—an illumination fiber and three collection fibers (core/cladding diameter of 50/60 μm)—that allowed for an angle-resolved backscattering measurement facilitating diffuse background correction (figure 3.II.(A)). Furthermore, a bevelled glass rod with 9.5° was placed at the tip of the probe (outer diameter of 3.4 mm) in order to minimize specular reflection. The researchers demonstrated the LEBS probe for pancreatic cancer screening by examination of duodenal mucosa during upper endoscopy on 41 patients [29]. By using the probe, test performance with sensitivity of 78%, specificity of 85%, and accuracy of 81% was achieved for *in vivo* identification of pancreatic adenocarcinoma. Backman's group also demonstrated the LEBS probe for colorectal cancer diagnosis from 619 patients that showed sensitivity of 88% and specificity of 72% for rectal adenoma identification [17].

Finally, Perelman *et al* developed a spatial gating light scattering spectroscopy (LSS) probe that can distinguish precancerous pancreas tissue from benign cysts during endoscopic ultrasound-guided fine-needle aspiration (EUS-FNA) procedures (figure 3.III.) [32]. The 0.45 mm outer diameter spatial gating probe (figure 3.III. left) consisted of seven 100 μm core diameter fibers. A fiber in the outer ring of the probe for illumination and three groups of collection fibers provided illumination-collection separations, S_{ic}, of 120, 220 and 240 μm. A probe-latching mechanism enabling precise extension and retraction of the probe through EUS-FNA needle with position-locking was also developed for improved clinical effectiveness and practicality. While the collection fiber at S_{ic} = 120 μm collected signal resulting in both single-scattering and multiple scattering, the other collection fiber at S_{ic} = 240 μm collected multiple scattering signal alone (figure 3.III. right panel c). This facilitated correction of multiple scattering (diffuse reflection) signal and allowed effective extraction of single-scattering signal containing meaningful diagnostic information (figure 3.III. right panel d). Perelman and colleagues demonstrated the LSS probe for prediction of the potential malignancy of pancreatic cystic lesions (e.g. benign, low-grade dysplasia, high-grade dysplasia) during EUS-FNA procedures on 25 patients. In total, 14 cysts were measured *in vivo* and 13 postoperatively, and overall, an accuracy of 95%, a sensitivity of 90%, and a specificity of 100% was achieved.

5.2. Examples of FS

FS can be used to discriminate healthy from diseased biological tissue, with healthy and diseased tissues possessing different endogenous fluorescent properties, or when fluorescent contrast agents, which are designed to stain diseased tissues, are used. There have been many examples of the use of fluorescent spectroscopy to discriminate between healthy and diseased tissues *ex vivo* published since the earliest report in the 1940s [98]. There have also been many examples of fluorescent point-based spectroscopy for diagnostic discrimination of healthy and diseased tissues in many parts of the anatomy, both in

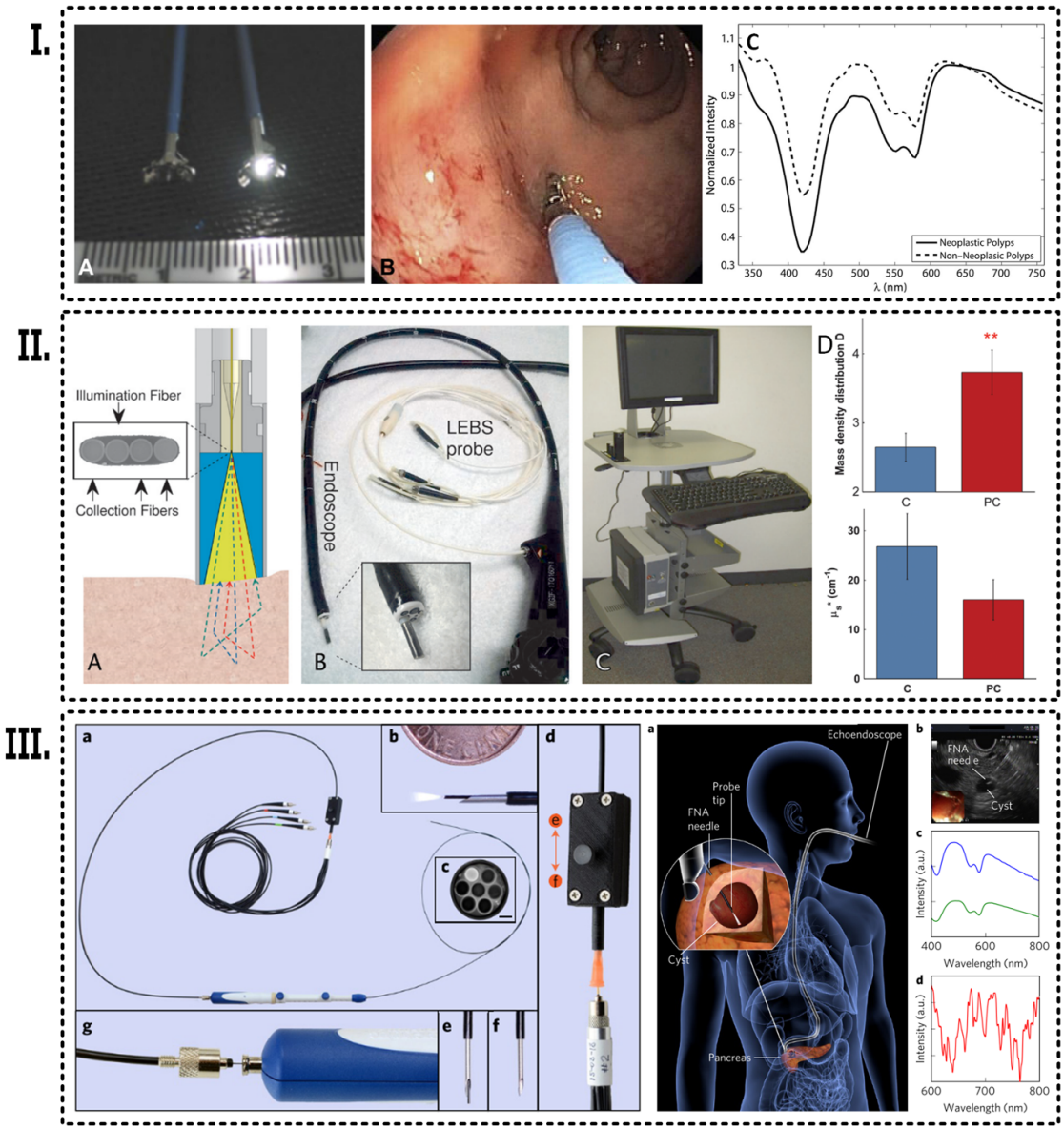


Figure 3. Examples of EOSS probes. **I.** ESS probe. (A) A photograph of standard biopsy forceps and forceps with an integrated dual-fiber probe for ESS. (B) Use of ESS integrated forceps for polyp assessment. (C) Representative ESS spectra for neoplastic polyps (solid line) and non-neoplastic polyps (dashed line). Reprinted from [93], Copyright (2014), with permission from Elsevier. **II.** LEBS probe. (A) A schematic of 3.4 mm diameter fiber-optic LEBS probe. (B) A photograph of the LEBS probe inserted into the accessory channel of an upper endoscope. (C) Portable cart used to house the data acquisition instrumentation and software for the LEBS probe. (D) Optical properties between control (C) and pancreatic adenocarcinomas (PC) extracted from the measurement results. Copyright © 2015 Wolters Kluwer Health, Inc. All rights reserved. **III.** Photographs of the spatial gating LSS probe inserted in the FNA needle and details of probe end, assembly, and probe latching mechanism (left). *In vivo* measurement during the endoscopic ultrasound-guided fine-needle aspiration (EUS-FNA) procedure and typical spectra collected in the cyst at 120 μm (blue) and 240 μm (green), and the backscattering component extracted from the spectra (red) (right). Copyright © 2017, Springer Nature.

developmental animal models and in human medical trials, including the alimentary tract [44, 99–130], heart or major arteries [131–141], bladder [142–149], brain [45–48, 143, 150–175], breast [176], cervix [177–194], endocrine system [195–201], head and neck [9, 202–213], kidneys [214–216], liver [217–224], lungs [143, 225–228], mesothelium [229], and the prostate [230].

One example of a fluorescence spectroscopy system in TRL Group C, which was used in a human medical trial, was the work of Neumann *et al* in which they assessed whether a commercial laser-induced fluorescence spectroscopic biopsy system could meet the performance thresholds, set by the ASGE, for accurate real-time assessment of histology of colorectal polyps [120, 124]. Real-time assessment of the histology of diminutive colorectal polyps would enable a reduction in the risks to patients, medical time and costs associated with polyp resection [231]. The commercial system used by Neumann *et al* was the WavSTAT4 system. The excitation wavelength was 337 nm. A total of 27 patients underwent screening colonoscopy and the histology

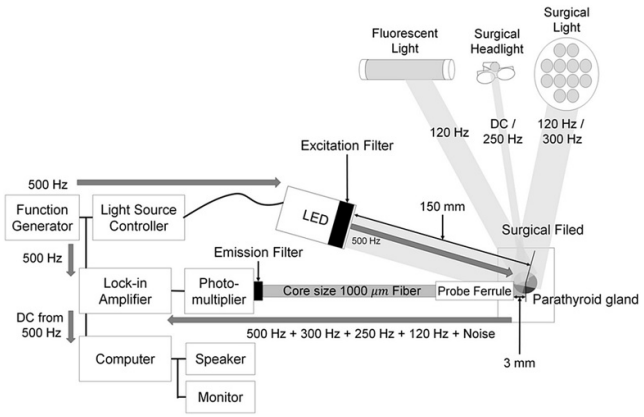


Figure 4. The PG sensor probe developed and tested by Kim *et al* used for discrimination of the parathyroid glands from the thyroid during thyroidectomy procedures. The function generator operating at 500 Hz and connected to the light source and detector enabled the phase-sensitive process. [201] John Wiley & Sons © 2019 WILEY-VCH Verlag GmbH & Co. KGaA, Weinheim.

of diminutive colorectal polyps (137 total) were determined *in vivo* and in real time using the light-induced fluorescence spectroscopy system. Diminutive polyps were determined to be 'not suspect' (benign) or 'suspect' (cancerous) using the proprietary algorithm in the software and these findings were compared to the results of the histopathological examination of the biopsied samples. Due to the small sample size in the study, with only 22 of the 137 polyps being adenomatous, the negative predictive value (NPV) may be deceptively high and further studies would be needed. In addition, the positive predictive value (PPV) was only 33% so this technique would not necessarily proclude histology. However, it was determined that the accuracy for predicting the length of time before another surveillance was needed (known as a surveillance interval) was nearly met, or even exceeded in some cases, the ASGE recommended thresholds.

Kim *et al* published a preliminary report on the use of a phase-sensitive NIR autofluorescence detector, dubbed the 'PG sensor' (TRL Group B), during thyroidectomy surgery [201]. The PG sensor probe set-up is shown in figure 4. The *in vivo* preliminary trial was operated in a non-contact manner, due to ethical permission constraints, but nonetheless enabled the surgeon to identify the parathyroid glands from the thyroid. The probe system managed to detect the weak autofluorescence from the parathyroid glands ($\lambda_{em} = 822$ nm) when exposed to the excitation light ($\lambda_{ex} = 785$ nm) and in the presence of bright fluorescent room lights, the surgeon's headlight and other surgical lights. This was achieved through use of a function generator, which modulated the excitation light power frequency output at 500 Hz, and which was also connected to the lock-in amplifier that was attached to the photomultiplier detector. This ensured that only light with the power frequency of 500 Hz was detected and other light with different power frequencies was removed. Subsequently, the lock-in amplifier produced a DC voltage output which was proportional to the intensity of autofluorescence light received, and this was coupled to a speaker. When a higher autofluorescence signal was detected, a fast tempo sound was generated, compared to a slow regular interval sound when no autofluorescence signal was detected. Therefore, based on the output sound, the surgeon could discriminate the parathyroid gland/s from the thyroid when sweeping the probe over the surgical field. This probe thus enabled the surgeon to be able to immediately determine the position of the parathyroid glands without having to pause the operation to use conventional fluorescence imaging techniques to visualize the parathyroid glands whilst in the dark. Furthermore, the authors of the study proposed in future work that a co-axial version of this probe with the same optical axis of illumination and detection used in contact mode could be suitable for MIS using telescopic or robotic endoscopy. It should be noted that a similar and competing technology for parathyroid gland detection by autofluorescence point spectroscopy, the PTeye, has also been designed and tested in larger scale initial clinical trials by the group of Mahadevan-Jansen [195, 197, 199].

Since the earliest human *in vivo* examples, the fluorescence spectroscopy technique has continued to be developed and one of the latest iterations of the technique is simultaneous time- and wavelength-resolved fluorescence spectroscopy (STWRFS). The STWRFS system was reported by Marcu *et al* and it allows for the recording of several fluorescence response pulses at selected wavelengths over a period of less than 200 ns using just a single detector and excitation source [232]. The STWRFS system enables dynamic acquisition of fluorescence lifetime data over several spectral bands, whilst moving the probe across biological tissue [140].

Marcu *et al* validated the use of STWRFS for characterization of arterial vessel tissue *in vivo* on pigs [140]. The STWRFS system was comprised of a pulsed nitrogen laser (repetition rate = 50 Hz, $\lambda = 337$ nm, pulse width = 700 ps) coupled into an optical fiber (Ø = 400 μm, NA = 0.22), which was also used to collect the fluorescence emitted light. In turn, the autofluorescence emitted light was delivered to a series of 45° dichroic filters and band-pass filters so that the light was split into three appropriate sub-bands corresponding to the autofluorescence of common components of arterial tissue, which Marcu and co-workers had established in their previous work [138, 233, 234]. The STWRFS *in vivo* scanning experiments were conducted, using the catheter pullback sequence method, intravascularly in either 'still' or 'scanning' test modes. It was shown that the STWRFS system was able to reliably record autofluorescence signals. More crucially, the independence of autofluorescence lifetime to factors that negatively affect fluorescent emission intensity based measurements was also demonstrated.

5.3. Examples of RS

In biomedical applications, RS has been actively demonstrated as a sensitive and non-destructive *in vivo* diagnostic technique for discrimination of abnormal tissues in the last few decades. Due to the easy accessibility, extensive trials have been carried out for upper and lower gastrointestinal tracts, such as mouth, esophagus, stomach [70, 74, 235–241], and small and large intestines [77, 80, 81, 242–244]. Other organs that have been reported include coronary arteries [72, 79, 245], cervix [75, 246–249], breast [250], respiratory system (lung, larynx, etc) [82, 251, 252], bladder [253], and brain [76, 254, 255].

EmVision, LLC is a successfully established manufacturer providing advanced optical systems for Raman spectroscopy, particularly for clinical applications. A lensed Raman probe, a miniature endoscopic Raman probe, and a multispectral probe are available as a result of over the last 10 years of investigation. The probes are bundles of coaxially arranged fibers with the filter elements at the tips. These filters are cut into desired shapes, a small disk of band pass filter for the central excitation fiber and a donut-like shape long pass filter for the surrounding collection fibers [256, 257]. Additionally, a two-component front lens is integrated at the distal ends of the probes to enhance overlapping the analytical volume (outer diameter < 2 mm). Diagnosis of abnormalities in coronary artery [258], brain [76, 254, 255], bowel [244], and cervix [75] has been demonstrated by several groups using these probes so far. Further advancement has been made by integrating the probe within robot-assisted surgery by Pinto *et al* in 2019 [259]. A Raman probe (2.5 mm in outer diameter) comprised of a single central excitation fiber (105 μm core diameter) surrounded by 12 fibers for detection was integrated within a da Vinci robot system (da Vinci Xi, Intuitive Surgical) (figure 5.I.). Prostate tissue discrimination among anatomical regions (i.e. anterior, extraprostatic, etc) was demonstrated for use in robot-assisted prostatectomy procedures. An accuracy, a sensitivity, and a specificity of 91%, 90.5%, and 96%, respectively, was achieved bv *ex vivo* (599 spectra from 20 patients) and *in vivo* (20 spectra from 4 patients) demonstrations.

The other probe that has achieved higher TRL level was initially developed by Huang *et al* [260] and constantly has been modified and demonstrated for different applications. The latest version of the probe was comprised of a flat central illumination fiber surrounded by 18 beveled collection fibers (all fibers were 200 μm in diameter) and a 1 mm sapphire ball lens (NA = 1.78) at the tip of the probe (1.8 mm in outer diameter) [261]. The combination of the beveled collection fibers and the ball lens facilitated an optimal light steering performance to achieve a confocal measurement capability. Furthermore, the researchers put extra efforts to reject unwanted wavelength by filtering at both the distal and proximal ends of the probe. They deposited dielectric filter coatings on to the end-facets of the optical fibers (band pass filter coating on the central illumination fiber and long pass filter coating on the surrounding collection fibers) as well as connected external filter modules at the proximal ends (a 785 nm band pass filter at the laser and a long pass filter at the detector). *In vivo* clinical trials using this probe on esophagus [239, 240], stomach [243, 262], colon [242] (figure 5.II.), and larynx [252] were demonstrated. For discrimination of tissue types (i.e. normal, benign and malignant tumor), preceding assessment of various classification algorithms, such as classification and regression tree (CART) [235], partial least squares discriminant analysis (PLS-DA) [73], non-negativity-constrained least squares minimization (NNCLSM) [236], and ant colony optimization integrated with linear discriminant analysis (ACO-LDA) [237], was carried out on human stomach with the earlier version of the probe (flat 1-to-32 excitation-to-collection fibers) [260]. Furthermore, a prototype of the clinical Raman endoscopy system (all-in-a mobile cart) in which diagnosis software based on the discrimination algorithms mentioned above is on board was successfully developed and demonstrated in the operating room in a real-time *in situ* manner [74, 238].

5.4. Multimodal spectroscopy

There are many examples of deep, *in vivo* and quasi-real-time multimodal optical diagnosis systems reported in the literature. The most common multimodal optical diagnosis type is FS combined with DRS

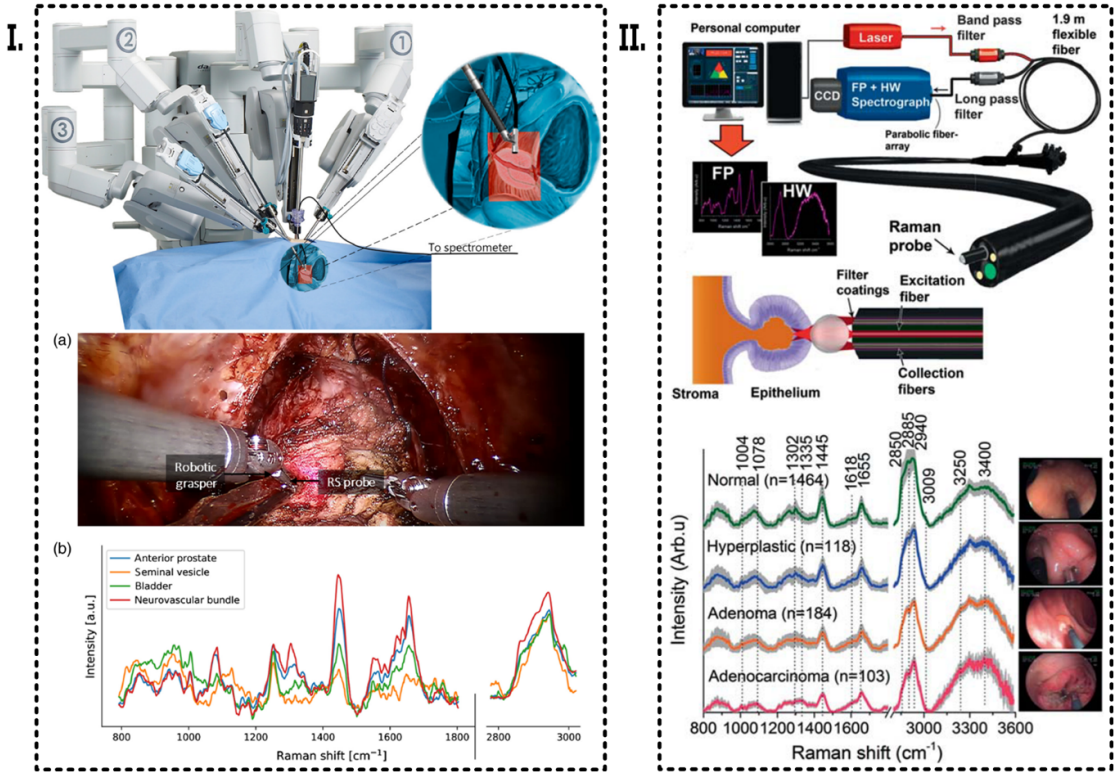


Figure 5. Examples of RS probes**. I.** The EmVision probe. Representation of the Raman spectroscopy probe integrated with the da Vinci robot-assisted surgical system composed of four independently controllable robotic arms (top). Closeup views of Raman spectroscopy probe during spectral acquisition on prostate base *in vivo* (middle). Mean spectra of specific tissue classes acquired *in vivo* (bottom). Reproduced from [259]. CC BY 4.0. **II.** The probe developed by Huang's group. The rapid simultaneous fingerprint (FP) and high-wavenumber (HW) fiber-optic Raman spectroscopy system for *in vivo* tissue diagnosis and characterization at colonoscopy (top). The mean FP/HW *in vivo* Raman spectra of normal, hyperplastic polyps, adenoma, and adenocarcinoma during colorectal endoscopy. Each spectrum was acquired within 0.1 to 0.5 s (bottom). [242] John Wiley & Sons. © 2016 WILEY-VCH Verlag GmbH & Co. KGaA, Weinheim.

(FS + DRS) [153, 175, 191, 263–291]. The other types are; FS plus RS plus DRS (FS + RS + DRS) [292–294], FS plus RS (FS + RS) [295, 296], FS plus DRS plus EOSS (FS + DRS + EOSS) [297–300] and FS combined with Doppler flowmetry (FS + Doppler flowmetry) [301–303]. These multimodal spectroscopy systems have been used on many different parts of the anatomy, including the alimentary tract, brain, cervix, endocrine system, head & neck (including oral and nasopharynx), heart and the liver.

In the work of Georgakoudi *et al*, it was demonstrated the use of a FS + DRS + EOSS multimodal spectroscopy system for evaluation of dysplasia in patients with Barrett's esophagus [299]. The system was based on the fast excitation-emission matrix (EEM) instrument that the authors had developed previously for a FS + DRS multimodal spectroscopy system for potential deep and *in vivo* diagnosis of colon tissues [276]. The fluorescence excitation light source of the EEM consisted of a 337 nm nitrogen laser which was used to pump 10 dye cuvettes that were mounted on a rapidly rotating wheel. Therefore, 11 different excitation wavelengths, between 337 and 620 nm, were obtained and coupled into the light delivery fiber of an optical fiber probe ($\varnothing = 1$ mm). For the DRS and EOSS reflectance measurements, white light (350–700 nm) from a xenon flash lamp was coupled into the same optical fiber probe. Six collection optical fibers surrounded the central light delivery optical fiber, and these fibers were used to collect the fluorescence emission and the reflected light from the tissue. The overall probe was covered with a transparent optical shield, which was used for protection. Overall, it was determined that the combination of the three modalities was superior to any of the techniques separately, in terms of the sensitivity and specificity of classification of the degree of dysplasia in Barrett's esophagus.

The LuViva™ system (vide supra) is a commercially available FS + DRS system, which is used for deep, *in vivo* and quasi-real-time investigation of the cervix [304]. The system consists of a hollow tube, which is inserted through a speculum into the vagina. The hollow tube is connected to a hand held device, which is used for spectral analysis and readout, and contains optics that transmit light from the broadband xenon arc lamp illumination source and collects the fluorescence emission and diffuse reflected light from the tissue. Werner *et al* used the LuViva™ system to compare the use of the point-based spectroscopy system (combined with additional cytology analysis) to human papilloma virus (HPV) testing for detection of high-grade

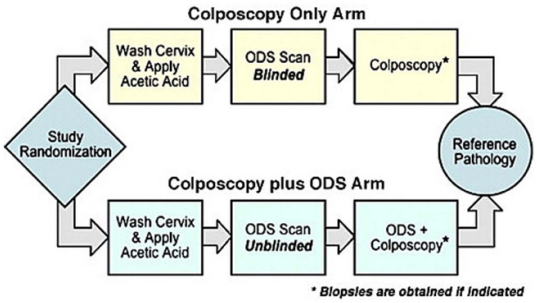


Figure 6. The two-arm study protocol used in the multicenter trial using the LUMA system. Reprinted from [263], Copyright (2007), with permission from Elsevier.

cervical neoplasia [280]. Light in the wavelength range 300 to 500 nm was used for fluorescence excitation and broadband light from 350 nm to 900 nm was used for DRS measurements. Wavelengths below 295 nm were filtered and blocked. The distal end of hollow tube was placed in intimate contact with the cervix for four minutes and fluorescent emission and diffuse reflected light from a plurality of equally spaced points over a 1 inch diameter area are analyzed by the system. Spectroscopic data was unavailable to the clinician and instead the LuViva™ system calculated spectroscopic indices which gave an indication to the clinician of the disease state of the cervix. A spectroscopy index (SI) of $1.5 \leq SI < 2.0$ indicated mild, moderate or severe dysplasia, $2.0 \leq SI < 2.5$ indicated the presence of atypical squamous cells of undetermined significance (ASC-US) and a $SI \geq 2.5$ indicated benign or normal cervical tissue. It was determined that point-based spectroscopy interrogation with the FS + DRS LuViva™ system plus cervical cytology was equally sensitive and doubly more specific than HPV testing plus cervical cytology ('co-testing') [280].

A competing commercially available system for deep, *in vivo* and quasi-real-time investigation of the cervix is the LUMA (vide supra) [266]. The system is used in a noncontact manner and consists of a scanning head, which is protected with disposable covers. Within the scanning head there are two xenon flash lamps for broadband white light for reflectance measurements, a 337 nm UV nitrogen laser for fluorescence spectroscopy and an endoscopic camera for visual imaging and to aid placement of the device. The FS + DRS light sources are coupled into a fiber-optic probe and the scanning head is held 10 cm from the cervix for a 12 s noncontact scan of the cervix. The scan area of the cervix is a 25 mm diameter circular area that is comprised of 499 scan points, which are spaced apart center-to-center ~1 mm and are also ~1 mm in diameter. Spectroscopic data is available to the clinician as spectra shown on the device console screen or as color overlays on images recorded with the camera. In one multicenter two-arm randomized trial, which compared colposcopy alone with colposcopy plus the LUMA system and consisted of 2299 women (see figure 6), there was a 26.5% gain in true-positives with the use of the LUMA system plus colposcopy. Thus it was determined that there was a clinically meaningful increase in the detection of cervical intraepithelial neoplasia grades 2, 3 through use of colposcopy with the LUMA system [263]. It should be noted that the LUMA device was not intended to replace colposcopy and is complimentary [266].

However, in terms of the use of multimodal spectroscopy systems for monitoring the cervix a comparison between the merits of optical spectroscopy systems versus standard of practise, must be assessed. For example, despite the use of the LuViva™ system plus cervical cytology being doubly more specific than 'co-testing' (HPV testing plus cervical cytology), the 'co-testing' Pap smear approach, when performed annually, is still highly successful as the progression of cervical cancer is very slow and thus neoplasia is regularly diagnosed at early and treatable stages [305].

6. Current status and future perspectives

6.1. Relative merits and challenges

As highlighted above, optical diagnosis systems allow for highly localized delivery and collection of light to and from tissues of clinical interest, which allows for optical diagnosis and facilitates an understanding of the specific biochemical processes that are occurring in the tissue. In addition to highly localized delivery of light, probe-based systems can be placed, and used, in areas of the body that are difficult to access, such as the thoracic wall [306]. However, spectroscopic measurements are typically performed at one or a few locations on the tissue and thus provide biochemical and/or structural information about the tissue with limited spatial resolution. Point-based optical diagnosis spectroscopic technologies allow for a wide spectral range to

be measured with a high spectral resolution, whereas if more spatial information is required then imaging modalities are more suited [307].

Generally, optical fibers are used in optical diagnosis systems and the typical diameters of optical fibers used are in the order of a couple of hundred microns and thus, even as a bundle, optical fibers are ideally suited to fit down the working channel of conventional endoscopes (Ø ~ 2.0 mm) [308]. Furthermore, optical fibers are generally made from silica and are relatively inexpensive, which allows for the optical fiber probes to be used in a disposable one-use manner. However, if required, optical fibers can be sterilized for reuse by the common medical sterilization methods [309].

In comparison to imaging techniques, optical diagnosis systems generally use technologies that are easier to implement, simpler to use and can be more portable than imaging systems [310]. Furthermore, to achieve performance that is cost-effective and in a timeframe that is clinically acceptable, spectral imaging techniques usually only focus on a few wavelengths or wavelength bands [307]. The accuracy and specificity of optical diagnosis has improved, and is continuing to improve for a wide range of pathological diseases and thus, an argument can be made that there is a clinical advantage of optical diagnosis.

However, the improved accuracy of optical diagnosis systems does not necessarily justify the use of systems in addition to, or in place of, standards of practise. For some diseases, such as cervical cancer (*vide supra*), despite the improvements in diagnosis accuracy afforded by an optical diagnosis system, the cost in terms of requiring expert users/practitioners of the system and extra clinical operation time burden may outweigh the benefits, compared to simpler histopathology diagnoses. In addition, there are concerns that, variations in measurement technique (e.g. the amount of pressure applied to the tissue when using a contact probe, etc) between different trained users could lead to operator-dependent errors and disparities in data collection and calibration. Indeed, it is for these reasons, and others, that there are currently only a limited number of optical spectroscopy technologies that have achieved routine use in clinical practise and most of these are pulse oximetry devices (which are excluded from the scope of this review) [307].

Finally, the monetary cost of these optical diagnosis systems may also be prohibitive to widespread use, with the systems costing more than simpler histopathological tests such as swab- or smear-based tests, such as the Pap smear. In comparison, extra additional monetary costs can be incurred through use of these systems, due to the possible burden of extra operating room time, which would result in increased anesthetic use and an increased anesthetist's clinical time. Economics is also a factor, as these technologies may be prohibitively expensive for roll-out in healthcare systems in developing economies, but on the whole, optical spectroscopy probe systems generally are cheaper than medical imaging systems [199].

It is clear that there are many advantages of optical diagnosis probe systems over histopathology biopsies and tests alone, but there are outstanding challenges to overcome the associated disadvantages of these techniques. For example, there is a need for more standardization of the many aspects of data collection using optical diagnosis systems, including calibration, positioning or posture of the patient, and also probe handling, including applied pressure when a probe is used in contact mode.

There is also a challenge to reduce the cost of these systems to make them more financially available. One way to potentially achieve this is to develop the probes, or parts of the probes, cheap enough so that parts of the probe assembly can be disposable or easily sterilizable. However, this subsequently raises the challenge of designing optical diagnosis systems so that some of the system parts can be used in a disposable/one-use manner, whilst at the same time allow for a clinical practitioner to be able to quickly and reproducibly reassemble the probe system with a new or sterilized part, with no impact on the operation and accuracy of the device.

Overall, optical diagnosis can be less invasive, less risky, and faster compared to conventional biopsy with histopathological diagnosis. There are challenges and unmet needs, but these provide opportunities to the biomedical engineering and biophotonics researcher communities.

6.2. Technical unmet needs and opportunities

Although the validity and usefulness of *in vivo* optical diagnosis technologies has been established in many clinical trials so far, further technical unmet needs still remain, such as miniaturization of the probes, performance, and implementation of *in vivo* diagnosis using the probes. First of all, there is a continuous demand for the further miniaturization of the diagnostic probes for more advanced and multi-functional MIS, flexible endoscopy, and natural orifice transluminal endoscopic surgery (NOTES). While submillimeter-scale outer diameters have been acquired with EOSS probes (0.45 mm outer diameter for the spatial gating LSS probe by Perelman *et al* [32] and 0.47 mm outer diameter for the ESS probe by Bigio *et al* [93]), FS/RS probes reported so far tend to be millimeter-scale because these probes usually require more collection fibers due to their inherently weaker signal intensity compared to EOSS. With further miniaturization of the probes, a reduction in the number of fibers will inevitably follow, and thus, this may deteriorate the detection performance. Moreover, integration of various optics at the tip of a probe that

improves the signal collection efficiency by focusing and conditioning the illumination/collection light (e.g. lenses, filters, polarizers, etc) becomes particularly harder when the probe gets smaller. Accordingly, development of novel technologies for probe fabrication and signal enhancement is required. Micro-to-mesoscale manufacturing technologies, e.g. laser machining, focused ion beam sputtering, etc, hold promise for development of next-generation optical diagnostic probes. Particularly, two-photon polymerization (2PP) technology, a microscale 3D printing technology, has demonstrated its value in fabrication of various microoptics and microtools at tips of optical fibers [311–315]. 2PP technology has also shown its capability of generating submicron-scale structures that can facilitate plasmonic surface-enhanced spectroscopies, such as SERS [316–318] and potentially metal-enhanced fluorescence (MEF). Furthermore, an optical fiber-based SERS probe was successfully developed by using 2PP technology for *in vitro* bacteria detection, which confirms that 2PP technology holds great potential for fabrication of novel diagnostic spectroscopy probes [319].

In addition to the demands of innovative fabrication technologies for probe development, further advancement in diagnostic algorithm models is required. Various machine learning techniques, e.g. support vector machine (SVM), artificial neural network (ANN), genetic algorithms (GA), etc, have been adopted as diagnostic algorithms for *in vivo* optical diagnosis and promising performance of these diagnostic algorithms has been demonstrated. Nevertheless, intrinsic technical shortcomings of machine learning techniques that influence the performance including limited applicability outside of the training dataset; tendency to be easily fooled due to biases; overfitting; and challenge of generalization to different populations, still remain as challenges [320]. Prospective cohort studies and randomized controlled trials (RCTs) will allow for elimination of some biases, will facilitate optimization of diagnostic algorithms based on the temporal observation of disease progression, and multiple different clinical outcomes in a large cohort of patients will improve comprehensive applicability [321]. These approaches will consequently allow for more reliable diagnostic algorithms and will eventually be able to open new opportunities for early diagnosis. The variable quality and transparency in reporting of published prediction models in medical research has raised difficulties for the scientific and healthcare communities in objective assessment and comparison of the models. To tackle this, transparent reporting of a multivariable prediction model for individual prognosis or diagnosis (TRIPOD) was developed. The TRIPOD statement was designed to support authors in writing reports describing the development, validation or updating of prediction models, aid editors and peer reviewers in reviewing manuscripts submitted for publication, and help readers in critically assessing published reports [322]. Moreover, a machine learning-specific TRIPOD statement (TRIPOD-ML) is currently in development to provide a tailored guideline, establishing methodological and reporting standards for studies of prediction algorithms based on machine learning in healthcare [323].

Great opportunities lie ahead in the field of vision-/robot-assisted surgeries and interventions combined with optical diagnosis technologies. Towards applications in MIS, flexible endoscopy, and NOTES, surgical tasks become particularly difficult and complex. Potential disadvantages of MIS include challenges in accurate guidance and navigation; limited operating space and field of vision; the lack of haptic feedback; the loss of stereo vision and depth perception; diminished hand-eye coordination; prolonged learning curves and training periods; extended operation times and increased costs [324]. Together with the latest high-resolution miniaturized cameras and recent progress in augmented reality and multimodal image registration technologies, such drawbacks are gradually being overcome. In addition, robotics can provide articulation, filtering of tremors, tactile sensing and haptic feedback, enhanced dexterity, and eye-hand coordination, which will improve surgical/diagnostic performances. There have been only very few early examples integrating optical diagnosis technologies with a robot-assisted surgical system (da Vinci Surgical System) [259, 325], and we expect that the attention and attempts to this approach will rapidly grow in the near future.

Finally, it is predicted that spectroscopy devices will incorporate optical sensors, which have been designed to be highly specific to certain disease biomarkers. As of yet, there are no optical fiber-based medical diagnostic biosensors that have been validated *in vivo* [326], but there is a clear opportunity for highly specific detection of biomarkers *in vivo* during optical diagnosis to be developed.

6.3. Clinical unmet needs and opportunities

Apart from the promising technical progress in optical diagnosis technologies, clinical unmet needs must be carefully analyzed when it comes to successful translation to clinics. Any new medical device must be approved by regulatory bodies, such as the FDA, in order to be introduced to clinics. Compact size, robustness, transportability of the device, and compatibility with existing systems are the key aspects that raise the likelihood of successful clinical translation [327]. Furthermore, user-friendliness is another crucial factor that determines the adoption in healthcare. Since the level of knowledge and expertise of the potential operators and interpreters of these emerging technologies (e.g. clinicians, nurses, technicians) may

significantly vary, developers are required to put themselves in the potential users' shoes throughout the development process. Participation of clinicians and the potential users in the development process from the early stage can direct the device development to the success in clinical translation by considering their advice and the user experience on prototypes.

Further clinical opportunities may lie in a wider range of target organs and diseases. Due to accessibility and different optical properties of different tissue types, there have been less investigations on specific target organs such as lung, brain, and breast in human *in vivo* (see section 4. Technology readiness levels (TRLs) and table 1). Optical diagnosis of diseases of these organs will, thus, bring huge impact and benefit more patients. Finally, liquid biopsies in oncology are emerging and their significance is gaining increasing attention. *In vivo*, real-time diagnosis of diseases from liquid biopsies—blood, biofluids, cerebrospinal fluid, pleural effusion, etc—will unlock the huge potential for early diagnosis of a broader range of diseases.

7. Conclusions

The interaction between incident light and biological tissue can provide much information about the nature and disease state of the tissue. The use of optical fiber-based probes allows for the highly localized application and collection of light to and from tissues of clinical interest (optical diagnosis) through utilization of conventional endoscopes. Optical diagnosis can be a less invasive, less risky, less costly and faster method compared to conventional tissue biopsy with histopathological diagnosis. The accuracy and specificity of optical diagnosis has improved and is continuing to improve for a wide range of pathological diseases and thus, the clinical advantage of optical diagnosis is evident, contributing to an increasingly important role in the future of healthcare provision. In addition, the further miniaturization of optical probes will allow for access to even smaller lumen within the body such as the terminal alveoli within the lungs, which are currently inaccessible to current standard bronchoscopes [328]. Furthermore, optical diagnosis is complementary to the advances in medical robotics and thus will have a growing role in the field of medical robotic diagnosis and surgery [329]. Finally, from a commercial point of view, the market of biophotonics is rapidly growing and the global biophotonics market is predicted to reach $63.1 billion by 2022 [330].

Overall, there is great scope for the future of the field of optical diagnosis to be bright.

Acknowledgments

The authors acknowledge funding from the UK Engineering and Physical Sciences Research Council (EPSRC) program grant EP/P012779/1 (Micro-Robotics for Surgery).

ORCID iDs

Jang Ah Kim https://orcid.org/0000-0002-8569-5512
Dominic J Wales https://orcid.org/0000-0003-3696-4867
Guang-Zhong Yang https://orcid.org/0000-0003-4060-4020

References

[1] Kayser K, Schultz H, Goldmann T, Görtler J, Kayser G and Vollmer E 2009 Theory of sampling and its application in tissue based diagnosis *Diagn. Pathol.* **4** 6
[2] Alshieban S and Al-Surimi K 2015 Reducing turnaround time of surgical pathology reports in pathology and laboratory medicine departments *BMJ Qual. Improv. Rep.* **4** u209223.w3773
[3] Wang T D and Van Dam J 2004 Optical biopsy: a new frontier in endoscopic detection and diagnosis *Clin. Gastroenterol. Hepatol.* **2** 744–53
[4] Suhalim J L, Boik J C, Tromberg B J and Potma E O 2012 The need for speed *J. Biophoton.* **5** 387–95
[5] Subramanian V and Ragunath K 2014 Advanced endoscopic imaging: a review of commercially available technologies *Clin. Gastroenterol. Hepatol.* **12** 368–76
[6] Coda S, Siersema P, Stamp G and Thillainayagam A 2015 Biophotonic endoscopy: a review of clinical research techniques for optical imaging and sensing of early gastrointestinal cancer *Endosc. Int. Open* **03** E380–92
[7] East J *et al* 2016 Advanced endoscopic imaging: European Society of Gastrointestinal Endoscopy (ESGE) technology review *Endoscopy* **48** 1029–45
[8] Hoffman A, Manner H, Rey J W and Kiesslich R 2017 A guide to multimodal endoscopy imaging for gastrointestinal malignancy—an early indicator *Nat. Rev. Gastroenterol. Hepatol.* **14** 421–34
[9] Majumder S K, Ghosh N, Kataria S and Gupta P K 2003 Nonlinear pattern recognition for laser-induced fluorescence diagnosis of cancer *Lasers Surg. Med.* **33** 48–56
[10] Ramírez-Elías M G and González F J 2018 Raman spectroscopy for *in vivo* medical diagnosis *Raman Spectroscopy* vol 395, ed G M Do Nascimento (Rijeka: InTech) pp 293–311

[11] Rodriguez-Diaz E, Castanon D A, Singh S K and Bigio I J 2011 Spectral classifier design with ensemble classifiers and misclassification-rejection: application to elastic-scattering spectroscopy for detection of colonic neoplasia *J. Biomed. Opt.* **16** 067009
[12] Pence I and Mahadevan-Jansen A 2016 Clinical instrumentation and applications of Raman spectroscopy *Chem. Soc. Rev.* **45** 1958–79
[13] Zhao J, Lui H, Lean D M and Zeng H 2007 Automated auto fluorescence background subtraction algorithm for biomedical Raman spectroscopy *Appl. Spectrosc.* **61** 1225–32
[14] Kumar R, Srivastava R and Srivastava S 2015 Detection and classification of cancer from microscopic biopsy images using clinically significant and biologically interpretable features *J. Med. Eng.* **2015** 1–14
[15] DeBerardinis R J and Chandel N S 2016 Fundamentals of cancer metabolism *Sci. Adv.* **2** e1600200
[16] Mahadevan-Jansen A and Richards-Kortum R R 1996 Raman spectroscopy for the detection of cancers and precancers *J. Biomed. Opt.* **1** 31–70
[17] Turzhitsky V, Qiu L, Itzkan I, Novikov A A, Kotelev M S, Getmanskiy M, Vinokurov V A, Muradov A V and Perelman L T 2014 Spectroscopy of scattered light for the characterization of micro and nanoscale objects in biology and medicine *Appl. Spectrosc.* **68** 133–54
[18] Jacques S L 2013 Optical properties of biological tissues: a review *Phys. Med. Biol.* **58** 37–61
[19] Wax A and Backman V 2009 *Biomedical Applications of Light Scattering* (New York: McGraw-Hill)
[20] Utzinger U and Richards-Kortum R R 2003 Fiber optic probes for biomedical optical spectroscopy *J. Biomed. Opt.* **8** 121
[21] Mutyal N N, Radosevich A, Gould B, Rogers J D, Gomes A, Turzhitsky V and Backman V 2012 A fiber optic probe design to measure depth- limited optical properties in-vivo with low-coherence enhanced backscattering (LEBS) spectroscopy *Opt. Express* **20** 19643
[22] Ho D, Drake T K, Bentley R C, Valea F A and Wax A 2015 Evaluation of hybrid algorithm for analysis of scattered light using ex vivo nuclear morphology measurements of cervical epithelium *Biomed. Opt. Express* **6** 2755
[23] Chang V T-C, Merisier D, Yu B, Walmer D K and Ramanujam N 2011 Towards a field-compatible optical spectroscopic device for cervical cancer screening in resource-limited settings: effects of calibration and pressure *Opt. Express* **19** 17908
[24] Schols R M, Alic L, Beets G L, Breukink S O, Wieringa F P and Stassen L P S 2015 Automated spectroscopic tissue classification in colorectal surgery *Surg. Innov.* **22** 557–67
[25] Myakov A, Nieman L, Wicky L, Utzinger U, Richards-Kortum R and Sokolov K 2002 Fiber optic probe for polarized reflectance spectroscopy *in vivo*: design and performance *J. Biomed. Opt.* **7** 388
[26] Chen P, Fernald B and Lin W 2011 Estimation of regional hemoglobin concentration in biological tissues using diffuse reflectance spectroscopy with a novel spectral interpretation algorithm *Phys. Med. Biol.* **56** 3985–4000
[27] Greening G, Mundo A, Rajaram N and Muldoon T J 2018 Sampling depth of a diffuse reflectance spectroscopy probe for in-vivo physiological quantification of murine subcutaneous tumor allografts *J. Biomed. Opt.* **23** 085006–14
[28] Radosevich A J *et al* 2015 Rectal optical markers for *in vivo* risk stratification of premalignant colorectal lesions *Clin. Cancer Res.* **21** 4347–55
[29] Mutyal N N *et al* 2015 *In vivo* risk analysis of pancreatic cancer through optical characterization of duodenal mucosa *Pancreas* **44** 735–41
[30] Mirabal Y N, Chang S K, Atkinson E N, Malpica A, Follen M and Richards-Kortum R 2002 Reflectance spectroscopy for *in vivo* detection of cervical precancer *J. Biomed. Opt.* **7** 587–94
[31] Oh S, Stewart T, Miller I, Bhatia S, Ragheb J, Duchowny M, Jayakar P and Lin W-C 2011 *In vivo* optical properties of cortical tubers in children with tuberous sclerosis complex (TSC): a preliminary investigation *Epilepsia* **52** 1699–704
[32] Zhang L *et al* 2017 Light scattering spectroscopy identifies the malignant potential of pancreatic cysts during endoscopy *Nat. Biomed. Eng.* **1** 0040
[33] Braslavsky S E 2007 Glossary of terms used in photochemistry, 3rd edition (IUPAC recommendations 2006) *Pure Appl. Chem.* **79** 293–465
[34] Lakowicz J R 2006 *Principles of Fluorescence Spectroscopy* (Boston, MA: Springer)
[35] Sauer M, Hofkens J and Enderlein J 2011 *Handbook of Fluorescence Spectroscopy and Imaging from Single Molecules to Ensembles* (New York: Wiley)
[36] Valeur B and Berberan-Santos M N 2013 *Molecular Fluorescence : Principles and Applications* (New York: Wiley)
[37] Haringsma J and Tytgat G N J 1999 Fluorescence and autofluorescence *Best Pract. Res. Clin. Gastroenterol.* **13** 1–10
[38] Durkin A J, Jaikumar S and Ramanujam N 1994 Spectra of dilute and turbid samples *Appl. Opt.* **33** 414–23
[39] Fanjul-Velez F and Arce-Diego J L 2011 Light propagation in turbid media: application to biological tissues *Proc. 21st Int. Conf. Radioelektronika 2011* (Piscataway, NJ: IEEE) pp 1–4
[40] Bradley R S and Thorniley M S 2006 A review of attenuation correction techniques for tissue fluorescence *J. R. Soc. Interface* **3** 1–13
[41] Sterenborg H J C M, Saarnak A E, Frank R and Motamedi M 1996 Evaluation of spectral correction techniques for fluorescence measurements on pigmented lesions *in vivo J. Photochem. Photobiol.* B **35** 159–65
[42] Chen Y, Chen Z-P, Yang J, Jin J-W, Zhang J and Yu R-Q 2013 Quantitative fluorescence spectroscopy in turbid media: a practical solution to the problem of scattering and absorption *Anal. Chem.* **85** 2015–20
[43] Wagnieres G A, Star W M and Wilson B C 1998 *In vivo* fluorescence spectroscopy and imaging for oncological applications *Photochem. Photobiol.* **68** 603–32
[44] Messmann H, Knüchel R, Endlicher E, Hauser T, Szeimies R M, Kullmann F, Bäumler W and Schölmerich J 1998 Photodynamische Diagnostik gastrointestinaler Präkanzerosen nach Sensibilisierung mit 5-Aminolävulinsäure: Eine Pilotstudie *Dtsch. Med. Wochenschr.* **123** 515–21
[45] Haj-Hosseini N, Richter J, Andersson-Engels S and Wårdell K 2010 Optical touch pointer for fluorescence guided glioblastoma resection using 5-aminolevulinic acid *Lasers Surg. Med.* **42** 9–14
[46] Haj-Hosseini N, Lowndes S, Salerud G and Wårdell K 2011 Blood interference in fiber-optical based fluorescence guided resection of glioma using 5-aminolevulinic acid *Proc. SPIE* **7883** 78833R
[47] Stummer W, Tonn J-C, Goetz C, Ullrich W, Stepp H, Bink A, Pietsch T and Pichlmeier U 2014 5-aminolevulinic acid-derived tumor fluorescence *Neurosurgery* **74** 310–20
[48] Valdes P A *et al* 2011 Quantitative fluorescence in intracranial tumor: implications for ALA-induced PpIX as an intraoperative biomarker *J. Neurosurg.* **115** 11–17
[49] Marcu L 2012 Fluorescence lifetime techniques in medical applications *Ann. Biomed. Eng.* **40** 304–31

[50] Raman C V and Krishnan K S 1928 A new type of secondary radiation *Nature* **121** 501–2
[51] Fini G 2004 Applications of Raman spectroscopy to pharmacy *J. Raman Spectrosc.* **35** 335–7
[52] Sikirzhytski V, Sikirzhytskaya A and Lednev I K 2011 Multidimensional Raman spectroscopic signatures as a tool for forensic identification of body fluid traces: a review *Appl. Spectrosc.* **65** 1223–32
[53] De Oliveira Penido C A F, Pacheco M T T, Lednev I K and Silveira L 2016 Raman spectroscopy in forensic analysis: identification of cocaine and other illegal drugs of abuse *J. Raman Spectrosc.* **47** 28–38
[54] Renishaw plc—Spectroscopy 2019 Using Raman spectroscopy in forensic science *AZoM* https://www.azom.com/article.aspx?ArticleID=11733 (Accessed: 17 June 2020)
[55] Fries M and Steele A 2011 Raman spectroscopy and confocal Raman imaging in mineralogy and petrography *Confocal Raman Microscopy*, ed T Dieing, O Hollricher and J Toporski (Berlin: Springer) pp 111–35
[56] Wang Y, Alsmeyer D C and Mccreery R L 1990 Raman spectroscopy of carbon materials: structural basis of observed spectra *Chem. Mater.* **2** 557–63
[57] Voronov O A and Street K W 2010 Raman scattering in a new carbon material *Diam. Relat. Mater.* **19** 31–39
[58] Bokobza L, Bruneel J-L and Couzi M 2014 Raman spectroscopy as a tool for the analysis of carbon-based materials (highly oriented pyrolitic graphite, multilayer graphene and multiwall carbon nanotubes) and of some of their elastomeric composites *Vib. Spectrosc.* **74** 57–63
[59] Tiberj A and Camassel J 2012 Raman imaging in semiconductor physics: applications to microelectronic materials and devices *Raman Imaging: Techniques and Applications* ed A Zoubir (Berlin: Springer) pp 39–83
[60] De Gelder J, De Gussem K, Vandenabeele P and Moens L 2007 Reference database of Raman spectra of biological molecules *J. Raman Spectrosc.* **38** 1133–47
[61] Butler H J *et al* 2016 Using Raman spectroscopy to characterize biological materials *Nat. Protoc.* **11** 664–87
[62] Shipp D W, Sinjab F and Notingher I 2017 Raman spectroscopy: techniques and applications in the life sciences *Adv. Opt. Photonics* **9** 315–428
[63] Movasaghi Z, Rehman S and Rehman I U 2007 Raman spectroscopy of biological tissues *Appl. Spectrosc. Rev.* **42** 493–541
[64] Kong K, Kendall C, Stone N and Notingher I 2015 Raman spectroscopy for medical diagnostics—from in-vitro biofluid assays to in-vivo cancer detection *Adv. Drug Deliv. Rev.* **89** 121–34
[65] Ding S-Y, Yi J, Li J-F, Ren B, Wu D-Y, Panneerselvam R and Tian Z-Q 2016 Nanostructure-based plasmon-enhanced Raman spectroscopy for surface analysis of materials *Nat. Rev. Mater.* **1** 16021
[66] De Luca A C, Dholakia K and Mazilu M 2015 Modulated Raman spectroscopy for enhanced cancer diagnosis at the cellular level *Sensors* **15** 13680–704
[67] Knorr F, Smith Z and Wachsmann-Hogiu S 2010 Development of a time-gated system for Raman spectroscopy of biological samples *Opt. Express* **18** 20049–58
[68] Hirschfeld T and Chase B 1986 FT-Raman spectroscopy: development and justification *Appl. Spectrosc.* **40** 133–7
[69] Puppels G J, van Aken M, Wolthuis R, Caspers P J, Bakker Schut T C, Bruining H A, Roemer T J, Buschman H P J, Wach M L and Robinson Jr J S 1998 In-vivo tissue characterization by Raman spectroscopy *Proc. SPIE* **3257** 78–83
[70] Shim M G, Song L-M W K, Marcon N E and Wilson B C 2000 *In vivo* near-infrared Raman spectroscopy: demonstration of feasibility during clinical gastrointestinal endoscopy *Photochem. Photobiol.* **72** 146–50
[71] Bakker Schut T C, Witjes M J H, Sterenborg H J C M, Speelman O C, Roodenburg J L N, Marple E T, Bruining H A and Puppels G J 2000 *In vivo* detection of dysplastic tissue by Raman spectroscopy *Anal. Chem.* **72** 6010–8
[72] Motz J T, Fitzmaurice M, Miller A, Gandhi S J, Haka A S, Galindo L H, Dasari R R, Kramer J R and Feld M S 2006 *In vivo* Raman spectral pathology of human atherosclerosis and vulnerable plaque *J. Biomed. Opt.* **11** 021003
[73] Bergholt M S, Zheng W, Lin K, Ho K Y, Teh M, Yeoh K G, Yan So J B and Huang Z 2010 Raman endoscopy for *in vivo* differentiation between benign and malignant ulcers in the stomach *Analyst* **135** 3162–8
[74] Duraipandian S, Bergholt M S, Zheng W, Ho K Y, Teh M, Yeoh K G, So J B Y, Shabbir A and Huang Z 2012 Real-time Raman spectroscopy for *in vivo*, online gastric cancer diagnosis during clinical endoscopic examination *J. Biomed. Opt.* **17** 081418
[75] O'Brien C M, Vargis E, Rudin A, Slaughter J C, Thomas G, Newton J M, Reese J, Bennett K A and Mahadevan-Jansen A 2018 *In vivo* Raman spectroscopy for biochemical monitoring of the human cervix throughout pregnancy *Am. J. Obstet. Gynecol.* **218** 528.e1–528.e18
[76] Desroches J *et al* 2018 A new method using Raman spectroscopy for *in vivo* targeted brain cancer tissue biopsy *Sci. Rep.* **8** 1792
[77] Taketani A, Andriana B B, Matsuyoshi H and Sato H 2017 Raman endoscopy for monitoring the anticancer drug treatment of colorectal tumors in live mice *Analyst* **142** 3680–8
[78] Mamun M A A L, Mahadevan-Jansen A, Juodkazis S and Stoddart P R 2018 Development of an optical fiber SERS microprobe for minimally invasive sensing applications *Proc. SPIE* **10501** 1
[79] Brennan J F, Wang Y, Dasari R R and Feld M S 1997 Near-infrared Raman spectrometer systems for human tissue studies *Appl. Spectrosc.* **51** 201–8
[80] Zavaleta C L, Garai E, Liu J T C, Sensarn S, Mandella M J, Van de Sompel D, Friedland S, Van Dam J, Contag C H and Gambhir S S 2013 A Raman-based endoscopic strategy for multiplexed molecular imaging *Proc. Natl Acad. Sci.* **110** E2288–97
[81] Garai E *et al* 2015 A real-time clinical endoscopic system for intraluminal, multiplexed imaging of surface-enhanced Raman scattering nanoparticles *PLoS One* **10** e0123185
[82] McGregor H C, Short M A, Lam S, Shaipanich T, Beaudoin E-L and Zeng H 2018 Development and *in vivo* test of a miniature Raman probe for early cancer detection in the peripheral lung *J. Biophoton.* **11** e201800055
[83] Das N K, Dai Y, Liu P, Hu C, Tong L, Chen X and Smith Z J 2017 Raman plus X: biomedical applications of multimodal Raman spectroscopy *Sensors* **17** 1592
[84] U.S. Department of Defence 2009 *Technology Readiness Assessment (TRA) Deskbook* U.S. Department of Defence
[85] Santos I P *et al* 2017 Raman spectroscopy for cancer detection and cancer surgery guidance: translation to the clinics *Analyst* **142** 3025–47
[86] Olechowski A, Eppinger S D and Joglekar N 2015 Technology readiness levels at 40: a study of state-of-the-art use, challenges, and opportunities *Portland Int. Conf. on Management of Engineering and Technology* vol 2015-Sept. (Piscataway, NJ: IEEE) pp 2084–94
[87] Johns M, Giller C A and Liu H 1998 Computational and *in vivo* investigation of optical reflectance from human brain to assist neurosurgery *J. Biomed. Opt.* **3** 437
[88] Lin W-C, Sandberg D I, Bhatia S, Johnson M, Oh S and Ragheb J 2010 Diffuse reflectance spectroscopy for *in vivo* pediatric brain tumor detection *J. Biomed. Opt.* **15** 061709

[89] Boyer J, Mourant J R and Bigio I J 1994 Theoretical and experimental investigations of elastic scattering spectroscopy as a potential diagnostic for tissue pathologies *Proc. OSA: Advances in Optical Imaging and Photon Migration* ed R R Alfano (Orlando, FL: Optical Society of America) pp 265–8
[90] Dhar A, Johnson K S, Novelli M R, Bown S G, Bigio I J, Lovat L B and Bloom S L 2006 Elastic scattering spectroscopy for the diagnosis of colonic lesions: initial results of a novel optical biopsy technique *Gastrointest. Endosc.* **63** 257–61
[91] Rodriguez-Diaz E, Bigio I J and Singh S K 2011 Integrated optical tools for minimally invasive diagnosis and treatment at gastrointestinal endoscopy *Robot. Comput. Integr. Manuf.* **27** 249–56
[92] Rodriguez-Diaz E, Atkinson C, Jepeal L I, Berg A, Huang C S, Cerda S R, O'Brien M J, Bigio I J, Farraye F A and Singh S K 2014 Elastic scattering spectroscopy as an optical marker of inflammatory bowel disease activity and subtypes *Inflamm. Bowel Dis.* **20** 1029–36
[93] Rodriguez-Diaz E, Huang Q, Cerda S R, O'Brien M J, Bigio I J and Singh S K 2015 Endoscopic histological assessment of colonic polyps by using elastic scattering spectroscopy *Gastrointest. Endosc.* **81** 539–47
[94] Lovat L B *et al* 2006 Elastic scattering spectroscopy accurately detects high grade dysplasia and cancer in Barrett's oesophagus *Gut* **55** 1078–83
[95] Pickard D C O, Bigio I J, Bown S G, Lovat L B, Ripley P M and Novelli M 2002 Optical biopsy for the diagnosis of dysplasia in Barrett's oesophagus *Proc. SPIE* **4613** 234–43
[96] Qiu L *et al* 2018 Multispectral light scattering endoscopic imaging of esophageal precancer *Light Sci. Appl.* **7** 17174
[97] Hu F *et al* 2014 Assessment of the sensitivity and specificity of tissue-specific-based and anatomical-based optical biomarkers for rapid detection of human head and neck squamous cell carcinoma *Oral Oncol.* **50** 848–56
[98] Moore G E, Peyton W T, French L and Walker W W 1948 The clinical use of fluorescein in neurosurgery - the localization of brain tumours *J. Neurosurg.* **5** 392–8
[99] Kapadia C R, Cutruzzola F W, O'Brien K M, Stetz M L, Enriquez R and Deckelbaum L I 1990 Laser-induced fluorescence spectroscopy of human colonic mucosa—detection of adenomatous transformation *Gastroenterology* **99** 150–7
[100] Cothren R M *et al* 1996 Detection of dysplasia at colonoscopy using laser-induced fluorescence: a blinded study *Gastrointest. Endosc.* **44** 168–76
[101] von Holstein C S, Nilsson A M, Andersson-Engels S, Willén R, Walther B and Svanberg K 1996 Detection of adenocarcinoma in Barrett's oesophagus by means of laser induced fluorescence *Gut* **39** 711–6
[102] Chen W, He B, Wei G H, Gao G and Li S 1996 Laser-induced fluorescence spectroscopy of human normal and cancerous tissues *Proc. SPIE* **2887** 156–61
[103] Vo-Dinh T, Panjehpour M, Overholt B F, Buckley III P F and Edwards D H 1996 Detection of colon malignancy using differential normalized fluorescence *Proc. SPIE* **2679** 26–33
[104] Panjehpour M, Overholt B, Vo-Dinh T, Haggitt R, Edwards D and Buckley F 1996 Endoscopic fluorescence detection of high-grade dysplasia in Barrett's esophagus *Gastroenterology* **111** 93–101
[105] Vo-Dinh T, Panjehpour M, Overholt B F and Buckley P 1997 Laser-induced differential fluorescence for cancer diagnosis without biopsy *Appl. Spectrosc.* **51** 58–63
[106] Chen W, He B and Wei G 1998 Ultraviolet laser-induced fluorescence spectroscopy diagnosis of human stomach malignant tissues *Lasers Med. Sci.* **13** 209–13
[107] Mycek M-A, Schomacker K T and Nishioka N S 1998 Colonic polyp differentiation using time-resolved autofluorescence spectroscopy *Gastrointest. Endosc.* **48** 390–4
[108] Vo-Dinh T, Panjehpour M and Overholt B F 1998 Laser-induced fluorescence for esophageal cancer and dysplasia diagnosisa *Ann. N. Y. Acad. Sci.* **838** 116–22
[109] Eker C, Montán S, Jaramillo E, Koizumi K, Rubio C, Andersson-Engels S, Svanberg K, Svanberg S and Slezak P 1999 Clinical spectral characterisation of colonic mucosal lesions using autofluorescence and δ aminolevulinic acid sensitisation *Gut* **44** 511–8
[110] Cothren R M *et al* 1990 Gastrointestinal tissue diagnosis by laser-induced fluorescence spectroscopy at endoscopy *Gastrointest. Endosc.* **36** 105–11
[111] Messmann H, Knüchel R, Bäumler W, Holstege A and Schölmerich J 1999 Endoscopic fluorescence detection of dysplasia in patients with Barrett's esophagus, ulcerative colitis, or adenomatous polyps after 5-aminolevulinic acid–induced protoporphyrin IX sensitization *Gastrointest. Endosc.* **49** 97–101
[112] Bourg-Heckly G, Blais J, Padilla -J-J, Bourdon O, Etienne J, Guillemin F and Lafay L 2000 Endoscopic ultraviolet-induced autofluorescence spectroscopy of the esophagus: tissue characterization and potential for early cancer diagnosis *Endoscopy* **32** 756–65
[113] Mayinger B, Horner P, Jordan M, Gerlach C, Horbach T, Hohenberger W and Hahn E G 2001 Light-induced autofluorescence spectroscopy for the endoscopic detection of esophageal cancer *Gastrointest. Endosc.* **54** 195–201
[114] Mayinger B, Jordan M, Horner P, Gerlach C, Muehldorfer S, Bittorf B R, Matzel K E, Hohenberger W, Hahn E G and Guenther K 2003 Endoscopic light-induced autofluorescence spectroscopy for the diagnosis of colorectal cancer and adenoma *J. Photochem. Photobiol.* B **70** 13–20
[115] Song J M *et al* 2003 Development of a fluorescence detection system using Optical Parametric Oscillator (OPO) laser excitation for *in vivo* diagnosis *Technol. Cancer Res. Treat.* **2** 515–23
[116] Pfefer T J, Paithankar D Y, Poneros J M, Schomacker K T and Nishioka N S 2003 Temporally and spectrally resolved fluorescence spectroscopy for the detection of high grade dysplasia in Barrett's esophagus *Lasers Surg. Med.* **32** 10–16
[117] Pfefer T J, Schomacker K T and Nishioka N S 2007 Long-term effects of photodynamic therapy on fluorescence spectroscopy in the human esophagus *Photochem. Photobiol.* **73** 664–8
[118] Panjehpour M, Overholt B F, Vo-Dinh T and Coppola D 2012 The effect of reactive atypia/inflammation on the laser-induced fluorescence diagnosis of non-dysplastic Barrett's esophagus *Lasers Surg. Med.* **44** 390–6
[119] Angelova L, Borisova E, Zhelyazkova A, Keremedchiev M, Vladimirov B and Avramov L 2013 Fluorescence spectroscopy of gastrointestinal tumors: in vitro studies and *in vivo* clinical applications *Proc. SPIE* **9032** 903209
[120] Rath T, Vieth M, Grauer M, Naegel A, Neurath M F and Neumann H 2015 *In vivo* real-time assessment of colorectal polyp histology using an optical biopsy forceps system based on laser-induced fluorescence spectroscopy [Abstract 626] *Gastrointest. Endosc.* **81** AB158
[121] Bjorkman D J, Samowitz W S, Brigham E J, Peterson B J and Straight R C 1991 Fluorescence localization of early colonic cancer in the rat by hematoporphyrin derivative *Lasers Surg. Med.* **11** 263–70

[122] Mohammed N, Sood R, Venkatachalapathy S, Abid F, Burr N, Meadows J, Carbonell J, Luthra P, Rotimi O and Subramanian V 2016 PTH-045a the accuracy of wavstat version 4 optical biopsy forceps in characterising colorectal polyps less 10 mm: a prospective blinded study: abstract PTH-045a table 1 *Gut* **65** A241
[123] Boerwinkel D F, Holz J A, Hawkins D M, Curvers W L, Aalders M C, Weusten B L, Visser M, Meijer S L and Bergman J J 2015 Fluorescence spectroscopy incorporated in an optical biopsy system for the detection of early neoplasia in Barrett's esophagus *Dis. Esophagus* **28** 345–51
[124] Rath T, Tontini G, Vieth M, Nägel A, Neurath M and Neumann H 2016 *In vivo* real-time assessment of colorectal polyp histology using an optical biopsy forceps system based on laser-induced fluorescence spectroscopy *Endoscopy* **48** 557–62
[125] Schomacker K T, Frisoli J K, Compton C C, Flotte T J, Richter J M, Deutsch T F and Nishioka N S 1992 Ultraviolet laser-induced fluorescence of colonic polyps *Gastroenterology* **102** 1155–60
[126] Schomacker K T, Frisoli J K, Compton C C, Flotte T J, Richter J M, Nishioka N S and Deutsch T F 1992 Ultraviolet laser-induced fluorescence of colonic tissue: basic biology and diagnostic potential *Lasers Surg. Med.* **12** 63–78
[127] Vo-Dinh T, Panjehpour M, Overholt B F, Farris C, Buckley F P and Sneed R 1995 *In vivo* cancer diagnosis of the esophagus using differential normalized fluorescence (DNF) indices *Lasers Surg. Med.* **16** 41–47
[128] Kolli V R, Shaha A R, Savage H E, Sacks P G, Casale M A and Schantz S P 1995 Native cellular fluorescence can identify changes in epithelial thickness in-vivo in the upper aerodigestive tract *Am. J. Surg.* **170** 495–8
[129] Kolli V R, Savage H E, Yao T J and Schantz S P 1995 Native cellular fluorescence of neoplastic upper aerodigestive mucosa *Arch. Otolaryngol.—Head Neck Surg.* **121** 1287–92
[130] Panjehpour M, Overholt B F, Schmidhammer J L, Farris C, Buckley P F and Vo-Dinh T 1995 Spectroscopic diagnosis of esophageal cancer: new classification model, improved measurement system *Gastrointest. Endosc.* **41** 577–81
[131] Bartorelli A L, Leon M B, Almagor Y, Prevosti L G, Swain J A, McIntosh C L, Neville R F, House M D and Bonner R F 1991 *In Vivo* human atherosclerotic plaque recognition by laser-excited fluorescence spectroscopy *J. Am. Coll. Cardiol.* **17** 160–8
[132] Asahara T *et al* 1993 Evaluation of multidirectional fluorescence-sensing laser catheter for the development of an intelligent laser angioplasty system *Proc. SPIE* **1878** 51–56
[133] Lagarto J, Dyer B T, Talbot C, Sikkel M B, Peters N S, French P M W, Lyon A R and Dunsby C 2015 Application of time-resolved autofluorescence to label-free *in vivo* optical mapping of changes in tissue matrix and metabolism associated with myocardial infarction and heart failure *Biomed. Opt. Express* **6** 324
[134] Morguet A J, Gabriel R E and Buchwald A B 1996 Experimental and clinical evaluation of a spectroscopy system for fluorescence-guided excimer laser angioplasty *Proc. SPIE* **2922** 454–9
[135] Morguet A J, Gabriel R E, Buchwald A B, Werner G S, Nyga R and Kreuzer H 1997 Single-laser approach for fluorescence guidance of excimer laser angioplasty at 308 nm: evaluation in vitro and during coronary angioplasty *Lasers Surg. Med.* **20** 382–93
[136] Miyagi M, Nakajima H, Katoh T, Usui M, Amemiya T, Nagai Y and Ibukiyama C 1999 Fluorescence spectrum analysis of atherosclerotic plaque using doxycycline *Jpn. Circ. J.* **63** 379–86
[137] Marcu L, Fang Q, Jo J A, Papaioannou T, Dorafshar A, Reil T, Qiao J-H, Baker J D, Freischlag J A and Fishbein M C 2005 *In vivo* detection of macrophages in a rabbit atherosclerotic model by time-resolved laser-induced fluorescence spectroscopy *Atherosclerosis* **181** 295–303
[138] Jo J A, Fang Q, Papaioannou T, Baker J D, Dorafshar A H, Reil T, Qiao J-H, Fishbein M C, Freischlag J A and Marcu L 2006 Laguerre-based method for analysis of time-resolved fluorescence data: application to in-vivo characterization and diagnosis of atherosclerotic lesions *J. Biomed. Opt.* **11** 021004
[139] Jo J *et al* 2007 New methods for time-resolved fluorescence spectroscopy data analysis based on the laguerre expansion technique—applications in tissue diagnosis *Methods Inf. Med.* **46** 206–11
[140] Sun Y, Sun Y, Stephens D, Xie H, Phipps J, Saroufeem R, Southard J, Elson D S and Marcu L 2011 Dynamic tissue analysis using time- and wavelength-resolved fluorescence spectroscopy for atherosclerosis diagnosis *Opt. Express* **19** 3890
[141] Papayan G V, Galagudza M M, Minasyan S M and Kishalov A A 2017 Spectrofluorimeter for estimating the metabolic state of organs and tissues *J. Opt. Technol.* **84** 843–50
[142] Baert L, Berg R, Van Damme B, D'Hallewin M-A, Johansson J, Svanberg K and Svanberg S 1993 Clinical fluorescence diagnosis of human bladder carcinoma following low dose photofrin injection *Urology* **41** 322–30
[143] Svanberg K *et al* 1994 Tissue characterization in some clinical specialities utilizing laser-induced fluorescence *Proc. SPIE* **2135** 2–15
[144] D'Hallewin M-A, Baert L and Vanherzeele H A 1995 In-vivo autofluorescence spectroscopy of bladder carcinoma with a mercury arc lamp *Proc. SPIE* **2387** 80–85
[145] Koenig F, McGovern F J, Althausen A F, Deutsch T F and Schomacker K T 1996 Laser induced autofluorescence diagnosis of bladder cancer *J. Urol.* **156** 1597–601
[146] Arendt J T, Levin H S, Klein E A, Manoharan R, Feld M S and Cothren R M 1997 Detection of early cancerous changes in bladdar tissue by autofluorescence *Proc. 19th Annual Int. Conf. of the IEEE Engineering in Medicine and Biology Society* (Piscataway, NJ: IEEE) pp 2290–3
[147] A'Amar O M, Guillemin F H, Begorre H and Yvroud E 1997 Autofluorescence spectroscopy of normal and pathological tissues of the bladder *Proc. SPIE* **3197** 41–49
[148] Koenig F, McGovern F J, Enquist H, Larne R, Deutsch T F and Schomacker K T 1998 Autofluorescence guided biopsy for the early diagnosis of bladder carcinoma *J. Urol.* **159** 1871–5
[149] Zaak D, Stepp H, Baumgartner R, Schneede P, Waidelich R, Frimberger D, Hartmann A, Knchel R, Hofstetter A and Hohla A 2002 Ultraviolet-excited (308 nm) autofluorescence for bladder cancer detection *Urology* **60** 1029–33
[150] Croce A C, Fiorani S, Locatelli D, Nano R, Ceroni M, Tancioni F, Giombelli E, Benericetti E and Bottiroli G 2003 Diagnostic potential of autofluorescence for an assisted intraoperative delineation of glioblastoma resection margins *Photochem. Photobiol.* **77** 309–18
[151] Crespi F, Croce A C, Fiorani S, Masala B, Heidbreder C and Bottiroli G 2004 *In vivo* autofluorescence spectrofluorometry of central serotonin *J. Neurosci. Methods* **140** 67–73
[152] Fang Q, Papaioannou T, Jo J A, Vaitha R, Shastry K and Marcu L 2004 Time-domain laser-induced fluorescence spectroscopy apparatus for clinical diagnostics *Rev. Sci. Instrum.* **75** 151–62
[153] Toms S A, Lin W-C, Weil R J, Johnson M D, Jansen E D and Mahadevan-Jansen A 2005 Intraoperative optical spectroscopy identifies infiltrating glioma margins with high sensitivity *Oper. Neurosurg.* **57** 382–91
[154] Li Y, Li M and Xu T 2006 Quantitative time-resolved fluorescence spectra of the cortical sarcoma and the adjacent normal tissue determined with an *in vivo* experimental method and theoretical model *Appl. Spectrosc.* **60** 808–12

[155] Croce A C, Pisu M B, Roda E, Avella D, Bernocchi G and Bottiroli G 2006 Autofluorescence properties of rat cerebellum cortex during postnatal development *Lasers Surg. Med.* **38** 598–607
[156] Li Y, Xu T, Guo H and Yang H 2007 Is phosphorescence lifetime an indicator of angiogenesis in cortical sarcoma? *J. Fluoresc.* **17** 437–43
[157] Lin W-C, Ragheb J, Bhatia S, Johnson M, Sandberg D, Fernandez A, Morrison G, Duchowny M and Jayakar P 2007 *In vivo* optical characterization of pediatric epileptogenic lesions *Proc. SPIE* **6424** 642427
[158] Ilias M A, Richter J, Westermark F, Brantmark M, Andersson-Engels S and Wårdell K 2007 Evaluation of a fiber-optic fluorescence spectroscopy system to assist neurosurgical tumor resections *Proc. SPIE* **6631** 66310W
[159] Majumder S K, Gebhart S, Johnson M D, Thompson R, Lin W-C and Mahadevan-Jansen A 2007 A probability-based spectroscopic diagnostic algorithm for simultaneous discrimination of brain tumor and tumor margins from normal brain tissue *Appl. Spectrosc.* **61** 548–57
[160] Li Y, Li M and Xu T 2007 Quantitative time-resolved fluorescence spectrum of the cortical sarcoma and the adjacent normal tissue *J. Fluoresc.* **17** 643–8
[161] Butte P V, Fang Q, Jo J A, Yong W H, Pikul B K, Black K L and Marcu L 2010 Intraoperative delineation of primary brain tumors using time-resolved fluorescence spectroscopy *J. Biomed. Opt.* **15** 027008
[162] Richter J C O, Haj-Hosseini N, Andersson-Engel S and Wårdell K 2011 Fluorescence spectroscopy measurements in ultrasonic navigated resection of malignant brain tumors *Lasers Surg. Med.* **43** 8–14
[163] Brydegaard M, Haj-Hosseini N, Wårdell K and Andersson-Engels S 2011 Photobleaching-insensitive fluorescence diagnostics in skin and brain tissue *IEEE Photonics J.* **3** 407–21
[164] Butte P V, Mamelak A N, Nuno M, Bannykh S I, Black K L and Marcu L 2011 Fluorescence lifetime spectroscopy for guided therapy of brain tumors *Neuroimage* **54** S125–35
[165] Liu Q, Grant G, Li J, Zhang Y, Hu F, Li S, Wilson C, Chen K, Bigner D and Vo-Dinh T 2011 Compact point-detection fluorescence spectroscopy system for quantifying intrinsic fluorescence redox ratio in brain cancer diagnostics *J. Biomed. Opt.* **16** 037004
[166] Ma D, Bec J, Gorpas D, Yankelevich D and Marcu L 2015 Technique for real-time tissue characterization based on scanning multispectral fluorescence lifetime spectroscopy (ms-TRFS) *Biomed. Opt. Express* **6** 987
[167] Vasefi F, Kittle D S, Nie Z, Falcone C, Patil C G, Chu R M, Mamelak A N, Black K L and Butte P V 2016 Intraoperative optical biopsy for brain tumors using spectro-lifetime properties of intrinsic fluorophores *Proc. SPIE* **9711** 97111T
[168] Richter J C O, Haj-Hosseini N, Hallbeck M and Wårdell K 2017 Combination of hand-held probe and microscopy for fluorescence guided surgery in the brain tumor marginal zone *Photodiagnosis Photodyn. Ther.* **18** 185–92
[169] Alston L M, Guyotat J, Mahieu-Williame L, Hebert M, Kantapareddy P, Meyronet D, Rousseau D and Montcel B 2017 Interventional fluorescence spectroscopy: preliminary results to detect tumor margins during glioma resection with two fluorescence spectra of PpIX *Proc. SPIE* **10411** 104110C
[170] Hartl B A, Ma H S W, Sridharan S, Hansen K S, Kent M S, Gorin F, Fragoso R C and Marcu L 2018 Label-free fluorescence lifetime spectroscopy detects radiation-induced necrotic changes in live brain in real-time *Biomed. Opt. Express* **9** 272–82
[171] Tsai J-C, Kao M-C and Hsiao Y-Y 1993 Fluorospectral study of the rat brain and glioma *in vivo Lasers Surg. Med.* **13** 321–31
[172] Bottiroli G F, Croce A C, Locatelli D, Nano R, Giombelli E, Messina A and Benericetti E 1998 Autofluorescence of normal and neoplastic human brain tissue: an aid for intraoperative delineation of tumor resection margins *Proc. SPIE* **3196** 183–91
[173] Bottiroli G, Croce A C, Locatelli D, Nano R, Giombelli E, Messina A and Benericetti E 1998 Brain tissue autofluorescence: an aid for intraoperative delineation of tumor resection margins *Cancer Detect. Prev.* **22** 330–9
[174] Bottiroli G F, Croce A C, Locatelli D, Lanza K S, Lebovitz E, Giombelli E and Benericetti E 1999 Further evidence of tissue autofluorescence potential for the intraoperative delineation of brain tumor resection margins *Proc. SPIE* **3567** 164–71
[175] Lin W-C, Toms S A, Johnson M, Jansen E D and Mahadevan-Jansen A 2007 *In vivo* brain tumor demarcation using optical spectroscopy *Photochem. Photobiol.* **73** 396–402
[176] Wach M L and Gervasio G J 1999 Fiber optic interface for laser spectroscopic Raman probes 9 US Patent 5,911,017
[177] Vansevičiūtė R, Venius J, Žukovskaja O, Kanopienė D, Letautienė S and Rotomskis R 2015 5-Aminolevulinic-acid-based fluorescence spectroscopy and conventional colposcopy for *in vivo* detection of cervical pre-malignancy *BMC Womens. Health* **15** 35
[178] Devi S, Panigrahi P K and Pradhan A 2014 Detecting cervical cancer progression through extracted intrinsic fluorescence and principal component analysis *J. Biomed. Opt.* **19** 127003
[179] Shi L, Shi S Q, Saade G R, Chwalisz K and Garfield R E 1999 Changes in cervical resistance and collagen fluorescence during gestation in rats *J. Perinat. Med.* **27** 188–94
[180] Garfield R E, Chwalisz K, Shi L, Olson G and Saade G R 1998 Instrumentation for the diagnosis of term and preterm labour *J. Perinat. Med.* **26** 413–36
[181] Koumantakis E, Vasileiou A, Makrigiannakis A, Unsöld E and Papazoglou T G 1997 Spectral variations of laser-induced tissue emission during *in vivo* detection of malignancies in the female genital tract *J. Photochem. Photobiol.* B **40** 183–6
[182] Ramanujam N, Mitchell M F, Mahadevan-Jansen A, Thomson S L, Staerkel G, Malpica A, Wright T, Atkinson N and Richards-Kortum R 1996 Cervical precancer detection using a multivariate statistical algorithm based on laser-induced fluorescence spectra at multiple excitation wavelengths *Photochem. Photobiol.* **64** 720–35
[183] Ramanujam N, Mitchell M F, Mahadevan A, Thomsen S, Malpica A, Wright T, Atkinson N and Kortum R R 1996 Spectroscopic diagnosis of cervical intraepithelial neoplasia (CIN) *in vivo* using laser-induced fluorescence spectra at multiple excitation wavlengths *Lasers Surg. Med.* **19** 63–74
[184] Glassman W, Bryam-Smith M and Garfield R E 1995 Changes in rat cervical collagen during gestation and after antiprogesterone treatment as measured *in vivo* with light-induced autofluorescence *Am. J. Obstet. Gynecol.* **173** 1550–6
[185] Richards-Kortum R, Mitchell M F, Ramanujam N, Mahadevan A and Thomsen S 1994 *In vivo* fluorescence spectroscopy: potential for non-invasive, automated diagnosis of cervical intraepithelial neoplasia and use as a surrogate endpoint biomarker *J. Cell. Biochem. Suppl.* **19** 111–9
[186] Ramanujam N, Mitchell M F, Mahadevan A, Warren S, Thomsen S, Silva E and Richards-Kortum R 1994 *In vivo* diagnosis of cervical intraepithelial neoplasia using 337-nm-excited laser-induced fluorescence *Proc. Natl Acad. Sci. USA* **91** 10193–7
[187] Yamal J-M, Zewdie G A, Cox D D, Neely Atkinson E, Cantor S B, MacAulay C, Davies K, Adewole I, Buys T P H and Follen M 2012 Accuracy of optical spectroscopy for the detection of cervical intraepithelial neoplasia without colposcopic tissue information; a step toward automation for low resource settings *J. Biomed. Opt.* **17** 047002

[188] Kuon R J, Shi S Q, Maul H, Sohn C, Balducci J, Shi L and Garfield R E 2011 A novel optical method to assess cervical changes during pregnancy and use to evaluate the effects of progestins on term and preterm labor *Am. J. Obstet. Gynecol.* **205** 82.e15–82.e20
[189] Schlembach D, Mackay L, Shi L, Maner W L, Garfield R E and Maul H 2009 Cervical ripening and insufficiency: from biochemical and molecular studies to *in vivo* clinical examination *Eur. J. Obstet. Gynecol. Reprod. Biol.* **144** S70–S76
[190] Fittkow C T, Maul H, Olson G, Martin E, MacKay L B, Saade G R and Garfield R E 2005 Light-induced fluorescence of the human cervix decreases after prostaglandin application for induction of labor at term *Eur. J. Obstet. Gynecol. Reprod. Biol.* **123** 62–66
[191] Huh W K *et al* 2004 Optical detection of high-grade cervical intraepithelial neoplasia *in vivo*: results of a 604-patient study *Am. J. Obstet. Gynecol.* **190** 1249–57
[192] Maul H, Olson G, Fittkow C T, Saade G R and Garfield R E 2003 Cervical light-induced fluorescence in humans decreases throughout gestation and before delivery: preliminary observations *Am. J. Obstet. Gynecol.* **188** 537–41
[193] Schlembach D, Maul H, Fittkow C, Olson G, Saade G and Garfield R 2003 Cross-linked collagen in the cervix of pregnant women with cervical insufficiency *Am. J. Obstet. Gynecol.* **189** S70
[194] Garfield R E, Maul H, Maner W, Fittkow C, Olson G, Shi L and Saade G R 2002 Uterine electromyography and light-induced fluorescence in the management of term and preterm labor *J. Soc. Gynecol. Investig.* **9** 265–75
[195] Paras C, Keller M, White L, Phay J and Mahadevan-Jansen A 2011 Near-infrared autofluorescence for the detection of parathyroid glands *J. Biomed. Opt.* **16** 067012
[196] McWade M A, Paras C, White L M, Phay J E, Mahadevan-Jansen A and Broome J T 2013 A novel optical approach to intraoperative detection of parathyroid glands *Surgery* **154** 1371–7
[197] McWade M A, Sanders M E, Broome J T, Solórzano C C and Mahadevan-Jansen A 2016 Establishing the clinical utility of autofluorescence spectroscopy for parathyroid detection *Surgery* **159** 193–203
[198] Thomas G *et al* 2018 Developing a clinical prototype to guide surgeons for intraoperative label-free identification of parathyroid glands in real time *Thyroid* **28** 1517–31
[199] Thomas G, McWade M A, Nguyen J Q, Sanders M E, Broome J T, Baregamian N, Solórzano C C and Mahadevan-Jansen A 2019 Innovative surgical guidance for label-free real-time parathyroid identification *Surgery* **165** 114–23
[200] Liu J, Wang X, Wang R, Xu C, Zhao R, Li H, Zhang S and Yao X 2020 Near-infrared auto-fluorescence spectroscopy combining with Fisher's linear discriminant analysis improves intraoperative real-time identification of normal parathyroid in thyroidectomy *BMC Surg.* **20** 4
[201] Kim Y, Kim S W, Lee K D and Ahn Y 2020 Phase-sensitive fluorescence detector for parathyroid glands during thyroidectomy: a preliminary report *J. Biophoton.* **13** e201960078
[202] Kumar P, Kanaujia S K, Singh A and Pradhan A 2019 *In vivo* detection of oral precancer using a fluorescence-based, in-house-fabricated device: a Mahalanobis distance-based classification *Lasers Med. Sci.* **34** 1243–51
[203] Majumder S K, Ghosh N and Gupta P K 2005 Relevance vector machine for optical diagnosis of cancer *Lasers Surg. Med.* **36** 323–33
[204] Eker C, Rydell R, Svanberg K and Andersson-Engels S 2001 Multivariate analysis of laryngeal fluorescence spectra recorded *in vivo* *Lasers Surg. Med.* **28** 259–66
[205] Schantz S P, Kolli V, Savage H E, Yu G, Shah J P, Harris D E, Katz A, Alfano R R and Huvos A G 1998 *In vivo* native cellular fluorescence and histological characteristics of head and neck cancer *Clin. Cancer Res.* **4** 1177–82
[206] Saito Nogueira M, Cosci A, Teixeira Rosa R G, Salvio A G, Pratavieira S and Kurachi C 2017 Portable fluorescence lifetime spectroscopy system for in-situ interrogation of biological tissues *J. Biomed. Opt.* **22** 1
[207] Sethupathi R, Gurushankar K and Krishnakumar N 2016 Optical redox ratio differentiates early tissue transformations in DMBA-induced hamster oral carcinogenesis based on autofluorescence spectroscopy coupled with multivariate analysis *Laser Phys.* **26** 116202
[208] Francisco A L N, Correr W R, Azevedo L H, Galletta V K, Pinto C A L, Kowalski L P and Kurachi C 2014 Fluorescence spectroscopy for the detection of potentially malignant disorders of the oral cavity: analysis of 30 cases *Laser Phys.* **24** 015701
[209] Francisco A L N, Correr W R, Pinto C A L, Filho J G, Chulam T C, Kurachi C and Kowalski L P 2014 Analysis of surgical margins in oral cancer using in situ fluorescence spectroscopy *Oral Oncol.* **50** 593–9
[210] Sun Y *et al* 2012 *In vivo* validation of a bimodal technique combining time-resolved fluorescence spectroscopy and ultrasonic backscatter microscopy for diagnosis of oral carcinoma *J. Biomed. Opt.* **17** 116003
[211] Liu J, Sun Y, Qi J and Marcu L 2012 A novel method for fast and robust estimation of fluorescence decay dynamics using constrained least-squares deconvolution with Laguerre expansion *Phys. Med. Biol.* **57** 843–65
[212] Lin K, Zheng W and Huang Z 2010 Integrated autofluorescence endoscopic imaging and point-wise spectroscopy for real-time *in vivo* tissue measurements *J. Biomed. Opt.* **15** 040507
[213] Majumder S K, Gupta A, Gupta S, Ghosh N and Gupta P K 2006 Multi-class classification algorithm for optical diagnosis of oral cancer *J. Photochem. Photobiol.* B **85** 109–17
[214] Tirapelli L F, Trazzi B F M, Bagnato V S, Tirapelli D P C, Kurachi C, da Costa M M, Tucci S, Cologna A J and Martins A C P 2009 Histopathology and laser autofluorescence of ischemic kidneys of rats *Lasers Med. Sci.* **24** 397–404
[215] Cassini M F, da Costa M M, Bagnato V S, Tirapelli L F, Silva G E B, Molina C A F, Martins A C P and Tucci S 2013 Fluorescence spectroscopy in renal ischemia and reperfusion: noninvasive evaluation of organ viability *Transplant. Proc.* **45** 1715–9
[216] Cassini M F, da Costa M M, Bagnato V S, Tirapelli L F, Silva G E B, Martins A C P and Tuccl S 2013 Evaluation by fluorescence spectroscopy of the most appropriate renal region for obtaining biopsies: a study in the rat *Transplant. Proc.* **45** 1761–5
[217] Rettig W, Strehmel B, Schrader S, Seifert H, Beuthan J and Minet O 1999 Fluorescence diagnosis in the border zone of liver tumors *Applied Fluorescence in Chemistry, Biology and Medicine* (Berlin: Springer) pp 537–51
[218] Anderson C D, Lin W-C, Beckham J, Mahadevan-Jansen A, Buttemere C R, Pierce J, Nicoud I B, Wright Pinson C and Chari R S 2004 Fluorescence spectroscopy accurately detects irreversible cell damage during hepatic radiofrequency ablation *Surgery* **136** 524–31
[219] Castro-e-silva O, Sankarankutty A K, Correa R B, Ferreira J, Vollet Filho J D, Kurachi C and Bagnato V S 2008 Autofluorescence spectroscopy in liver transplantation: preliminary results from a pilot clinical study *Transplant. Proc.* **40** 722–5
[220] De Oliveira G R, Sankarankutty A K, Castro E Silva O, Ferreira J, Kurachi C, Zucoloto S, Vannucchi H, Jordão A A, Marchini J S and Bagnato V S 2009 Fluorescence spectroscopy to diagnose hepatic steatosis in a rat model of fatty liver *Liver Int.* **29** 331–6
[221] Croce A C, Ferrigno A, Piccolini V M, Tarantola E, Boncompagni E, Bertone V, Milanesi G, Freitas I, Vairetti M and Bottiroli G 2014 Integrated autofluorescence characterization of a modified-diet liver model with accumulation of lipids and oxidative stress *Biomed Res. Int.* **2014** 803491

[222] Vollet Filho J D, da Silveira M R, Castro-e-silva O, Bagnato V S and Kurachi C 2015 Fluorescence spectroscopy for assessment of liver transplantation grafts concerning graft viability and patient survival *Proc. SPIE* **9531** 95310X
[223] Nazeer S S, Saraswathy A, Shenoy S J and Jayasree R S 2018 Fluorescence spectroscopy as an efficient tool for staging the degree of liver fibrosis: an *in vivo* comparison with MRI *Sci. Rep.* **8** 10967
[224] Croce A C, Ferrigno A, Bottiroli G and Vairetti M 2018 Autofluorescence-based optical biopsy: an effective diagnostic tool in hepatology *Liver Int.* **38** 1160–74
[225] Braun F, Schalk R, Nachtmann M, Hien A, Frank R, Beuermann T, Methner F-J, Kränzlin B, Rädle M and Gretz N 2019 A customized multispectral needle probe combined with a virtual photometric setup for *in vivo* detection of Lewis lung carcinoma in an animal model *Meas. Sci. Technol.* **30** 104001
[226] Bard M P L, Amelink A, Skurichina M, Noordhoek Hegt V, Duin R P W, Sterenborg H J C M, Hoogsteden H C and Aerts J G J V 2006 Optical spectroscopy for the classification of malignant lesions of the bronchial tree *Chest* **129** 995–1001
[227] Kusunoki Y, Imamura F, Uda H, Mano M and Horai T 2000 Early detection of lung cancer with laser-induced fluorescence endoscopy and spectrofluorometry *Chest* **118** 1776–82
[228] Hung J, Lam S, Leriche J C and Palcic B 1991 Autofluorescence of normal and malignant bronchial tissue *Lasers Surg. Med.* **11** 99–105
[229] Colasanti A, Kisslinger A, Fabbrocini G, Liuzzi R, Quarto M, Riccio P, Roberti G and Villani F 2000 MS-2 fibrosarcoma characterization by laser induced autofluorescence *Lasers Surg. Med.* **26** 441–8
[230] Werahera P N, Jasion E A, Yongjun L, Daily J W, Arangua P, Jones C, Nash S R, Morrell M and Crawford E D 2015 Human feasibility study of fluorescence spectroscopy guided optical biopsy needle for prostate cancer diagnosis *2015 37th Annual Int. Conf. of the IEEE Engineering in Medicine and Biology Society (EMBC)* pp 7358–61
[231] Rex D K *et al* 2011 The American society for gastrointestinal endoscopy PIVI (preservation and incorporation of valuable endoscopic innovations) on real-time endoscopic assessment of the histology of diminutive colorectal polyps *Gastrointest. Endosc.* **73** 419–22
[232] Sun Y, Liu R, Elson D S, Hollars C W, Jo J A, Park J, Sun Y and Marcu L 2008 Simultaneous time- and wavelength-resolved fluorescence spectroscopy for near real-time tissue diagnosis *Opt. Lett.* **33** 630
[233] Marcu L, Fishbein M C, Maarek J I and Grundfest W S 2001 Discrimination of human coronary artery atherosclerotic fluorescence spectroscopy *Arter. Thromb. Vasc. Biol.* **21** 1244–50
[234] Marcu L, Jo J A, Fang Q, Papaioannou T, Reil T, Qiao J-H, Baker J D, Freischlag J A and Fishbein M C 2009 Detection of rupture-prone atherosclerotic plaques by time-resolved laser-induced fluorescence spectroscopy *Atherosclerosis* **204** 156–64
[235] Huang Z, Teh S K, Zheng W, Lin K, Ho K Y, Teh M and Yeoh K G 2010 *In vivo* detection of epithelial neoplasia in the stomach using image-guided Raman endoscopy *Biosens. Bioelectron.* **26** 383–9
[236] Bergholt M S, Zheng W, Lin K, Ho K Y, Teh M, Yeoh K G, So J B Y and Huang Z 2011 Characterizing variability in *in vivo* Raman spectra of different anatomical locations in the upper gastrointestinal tract toward cancer detection *J. Biomed. Opt.* **16** 037003
[237] Bergholt M S, Zheng W, Lin K, Ho K Y, Teh M, Yeoh K G, Yan So J B and Huang Z 2011 *In vivo* diagnosis of gastric cancer using Raman endoscopy and ant colony optimization techniques *Int. J. Cancer* **128** 2673–80
[238] Bergholt M S, Zheng W, Ho K Y, Teh M, Yeoh K G, So J B Y, Shabbir A and Huang Z 2013 Fiber-optic Raman spectroscopy probes gastric carcinogenesis *in vivo* at endoscopy *J. Biophoton.* **6** 49–59
[239] Bergholt M S, Zheng W, Ho K Y, Teh M, Yeoh K G, Yan So J B, Shabbir A and Huang Z 2014 Fiberoptic confocal Raman spectroscopy for real-time *in vivo* diagnosis of dysplasia in Barrett's esophagus *Gastroenterology* **146** 27–32
[240] Wang J, Lin K, Zheng W, Ho K Y, Teh M, Yeoh K G and Huang Z 2015 Simultaneous fingerprint and high-wavenumber fiber-optic Raman spectroscopy improves *in vivo* diagnosis of esophageal squamous cell carcinoma at endoscopy *Sci. Rep.* **5** 12957
[241] Hattori Y, Komachi Y, Asakura T, Shimosegawa T, Kanai G I, Tashiro H and Sato H 2007 *In vivo* Raman study of the living rat esophagus and stomach using a micro-Raman probe under an endoscope *Appl. Spectrosc.* **61** 579–84
[242] Bergholt M S *et al* 2016 Simultaneous fingerprint and high-wavenumber fiber-optic Raman spectroscopy enhances real-time *in vivo* diagnosis of adenomatous polyps during colonoscopy *J. Biophoton.* **9** 333–42
[243] Lin K, Wang J, Zheng W, Ho K Y, Teh M, Yeoh K G and Huang Z 2016 Rapid fiber-optic Raman spectroscopy for real-time *in vivo* detection of gastric intestinal metaplasia during clinical gastroscopy *Cancer Prev. Res.* **9** 476–83
[244] Pence I J, Beaulieu D B, Horst S N, Bi X, Herline A J, Schwartz D A and Mahadevan-Jansen A 2017 Clinical characterization of *in vivo* inflammatory bowel disease with Raman spectroscopy *Biomed. Opt. Express* **8** 524
[245] Buschman H P, Marple E T, Wach M L, Bennett B, Bakker Schut T C, Bruining H A, Bruschke A V, Der Van Laarse A and Puppels G J 2000 *In vivo* determination of the molecular composition of artery wall by intravascular Raman spectroscopy *Anal. Chem.* **72** 3771–5
[246] Utzinger U, Heintzelman D L, Mahadevan-Jansen A, Malpica A, Follen M and Richards-Kortum R 2001 Near-infrared Raman spectroscopy for *in vivo* detection of cervical precancers *Appl. Spectrosc.* **55** 955–9
[247] Robichaux-Viehoever A, Kanter E, Shappell H, Billheimer D, Jones H and Mahadevan-Jansen A 2007 Characterization of Raman spectra measured *in vivo* for the detection of cervical dysplasia *Appl. Spectrosc.* **61** 986–93
[248] Mo J, Zheng W, Low J J H, Ng J, Ilancheran A and Huang Z 2009 High wavenumber Raman spectroscopy for *in vivo* detection of cervical dysplasia *Anal. Chem.* **81** 8908–15
[249] Duraipandian S, Zheng W, Ng J, Low J J H, Ilancheran A and Huang Z 2011 *In vivo* diagnosis of cervical precancer using Raman spectroscopy and genetic algorithm techniques *Analyst* **136** 4328–36
[250] Haka A S, Volynskaya Z, Gardecki J A, Nazemi J, Lyons J, Hicks D, Fitzmaurice M, Dasari R R, Crowe J P and Feld M S 2006 *In vivo* margin assessment during partial mastectomy breast surgery using Raman spectroscopy *Cancer Res.* **66** 3317–22
[251] Short M A, Lam S, McWilliams A, Zhao J, Lui H and Zeng H 2008 Development and preliminary results of an endoscopic Raman probe for potential *in vivo* diagnosis of lung cancers *Opt. Lett.* **33** 711–3
[252] Lin K, Zheng W, Lim C M and Huang Z 2016 Real-time *in vivo* diagnosis of laryngeal carcinoma with rapid fiber-optic Raman spectroscopy *Biomed. Opt. Express* **7** 3705
[253] Draga R O P, Grimbergen M C M, Vijverberg P L M, Swol C F P, Van Jonges T G N, Kummer J A and Ruud Bosch J L H 2010 *In vivo* bladder cancer diagnosis by high-volume Raman spectroscopy *Anal. Chem.* **82** 5993–9
[254] Jermyn M, Mok K, Mercier J, Desroches J, Pichette J, Saint-Arnaud K, Bernstein L, Guiot M C, Petrecca K and Leblond F 2015 Intraoperative brain cancer detection with Raman spectroscopy in humans *Sci. Transl. Med.* **7** 274ra19
[255] Desroches J *et al* 2015 Characterization of a Raman spectroscopy probe system for intraoperative brain tissue classification *Biomed. Opt. Express* **6** 2380

[256] Agenant M, Grimbergen M, Draga R, Marple E, Bosch R and Van Swol C 2014 Clinical superficial Raman probe aimed for epithelial tumor detection : phantom model results *Biomed. Opt. Express* **5** 8908–15
[257] Marple E T and Urmey K D 2014 Filtered fiber optic probe US Patent 8,702,321 B2
[258] Matthäus C, Dochow S, Bergner G, Lattermann A, Romeike B F M, Marple E T, Krafft C, Dietzek B, Brehm B R and Popp J 2012 *In vivo* characterization of atherosclerotic plaque depositions by Raman-probe spectroscopy and in vitro coherent anti-stokes Raman scattering microscopic imaging on a rabbit model *Anal. Chem.* **84** 7845–51
[259] Pinto M *et al* 2019 Integration of a Raman spectroscopy system to a robotic-assisted surgical system for real-time tissue characterization during radical prostatectomy procedures *J. Biomed. Opt.* **24** 1
[260] Huang Z, Teh S K, Zheng W, Mo J, Lin K, Shao X, Ho K Y, Teh M and Yeoh K G 2009 Integrated Raman spectroscopy and trimodal wide-field imaging techniques for real-time *in vivo* tissue Raman measurements at endoscopy *Opt. Lett.* **34** 758
[261] Wang J, Bergholt M S, Zheng W and Huang Z 2013 Development of a beveled fiber-optic confocal Raman probe for enhancing *in vivo* epithelial tissue Raman measurements at endoscopy *Opt. Lett.* **38** 2321–3
[262] Wang J, Lin K, Zheng W, Ho K Y, Teh M, Yeoh K G and Huang Z 2016 Fiber-optic Raman spectroscopy for: *in vivo* diagnosis of gastric dysplasia *Faraday Discuss.* **187** 377–92
[263] Alvarez R D, Wright T C and The Optical Detection Group 2007 Effective cervical neoplasia detection with a novel optical detection system: a randomized trial *Gynecol. Oncol.* **104** 281–9
[264] Alvarez R D, Wright T C and The Optical Detection Group 2007 Increased detection of high-grade cervical intraepithelial neoplasia utilizing an optical detection system as an adjunct to colposcopy *Gynecol. Oncol.* **106** 23–28
[265] Huh W K and The Optical Detection Group 2005 Optical detection of cervical neoplasia: results from an internally-controlled multicenter study *Gynecol. Oncol.* **99** S53
[266] Kendrick J E, Huh W K and Alvarez R D 2007 LUMA^{TM} cervical imaging system *Expert Rev. Med. Devices* **4** 121–9
[267] Dremin V V *et al* 2019 Optical fine-needle aspiration biopsy in a rat model *Proc. SPIE* **10877** 108770K
[268] Lagarto J L, Dyer B T, Peters N S, French P M W, Dunsby C and Lyon A R 2019 *In vivo* label-free optical monitoring of structural and metabolic remodeling of myocardium following infarction *Biomed. Opt. Express* **10** 3506
[269] Valdés P A, Kim A, Leblond F, Conde O M, Harris B T, Paulsen K D, Wilson B C and Roberts D W 2011 Combined fluorescence and reflectance spectroscopy for *in vivo* quantification of cancer biomarkers in low- and high-grade glioma surgery *J. Biomed. Opt.* **16** 116007
[270] Pery E, Blondel W C P M, Tindel S, Ghribi M, Leroux A and Guillemin F 2014 Spectral features selection and classification for bimodal optical spectroscopy applied to bladder cancer *in vivo* diagnosis *IEEE Trans. Biomed. Eng.* **61** 207–16
[271] Wade R, Spackman E, Corbett M, Walker S, Light K, Naik R, Sculpher M and Eastwood A 2013 Adjunctive colposcopy technologies for examination of the uterine cervix—DySIS, LuViva advanced cervical scan and Niris imaging system: a systematic review and economic evaluation *Health Technol. Assess. (Rockv.)* **17** v–240
[272] Jayanthi J L, Subhash N, Stephen M, Philip E K and Beena V T 2011 Comparative evaluation of the diagnostic performance of autofluorescence and diffuse reflectance in oral cancer detection: a clinical study *J. Biophoton.* **4** 696–706
[273] Schwarz R A, Gao W, Daye D, Williams M D, Richards-Kortum R and Gillenwater A M 2008 Autofluorescence and diffuse reflectance spectroscopy of oral epithelial tissue using a depth-sensitive fiber-optic probe *Appl. Opt.* **47** 825
[274] Schwarz R A, Gao W, Redden Weber C, Kurachi C, Lee J J, El-Naggar A K, Richards-Kortum R and Gillenwater A M 2009 Noninvasive evaluation of oral lesions using depth-sensitive optical spectroscopy *Cancer* **115** 1669–79
[275] Anand S, Cicchi R, Fantechi R, Gacci M, Nesi G, Carini M and Pavone F S 2017 Multimodal fiber-probe spectroscopy for the diagnostics and classification of bladder tumors *Proc. SPIE* **10038** 100380J
[276] Zângaro R A, Silveira L, Manoharan R, Zonios G, Itzkan I, Dasari R R, Van Dam J and Feld M S 1996 Rapid multiexcitation fluorescence spectroscopy system for *in vivo* tissue diagnosis *Appl. Opt.* **35** 5211
[277] Ferris D G, Dickman E D, Litaker M S, Smith K M, Allmond L M and Arrington T L 2003 Patient acceptance of fluorescent and reflective spectroscopy as a replacement test for the pap smear *J. Low. Genit. Tract Dis.* **7** 294–8
[278] Ferris D G, Litaker M S, Dickman E D, Allmond L M, Smith K M and Arrington T L 2003 Women's responses to cervical interrogation by fluorescent and reflective spectroscopy *J. Low. Genit. Tract Dis.* **7** 299–303
[279] Twiggs L B, Chakhtoura N A, Ferris D G, Flowers L C, Winter M L, Sternfeld D R, Lashgari M, Burnett A F, Raab S S and Wilkinson E J 2013 Multimodal hyperspectroscopy as a triage test for cervical neoplasia: pivotal clinical trial results *Gynecol. Oncol.* **130** 147–51
[280] Werner C L, Griffith W F, Ashfaq R, Gossett D, Wilkinson E, Raab S, Bambot S, Mongin D and Faupel M 2007 Comparison of human papilloma virus testing and spectroscopy combined with cervical cytology for the detection of high-grade cervical neoplasia *J. Low. Genit. Tract Dis.* **11** 73–79
[281] Nemkovich N A, Sobchuk A N, Rubinov A N, Kruchenok Y V, Shan'ko Y G and Chukhonskiĭ A I 2014 System for the optical diagnosis of tumors, and using it to identify pituitary adenoma *J. Opt. Technol.* **81** 578
[282] Yadav N, Bhatia S, Ragheb J, Mehta R, Jayakar P, Yong W and Lin W-C 2013 *In vivo* detection of epileptic brain tissue using static fluorescence and diffuse reflectance spectroscopy *J. Biomed. Opt.* **18** 027006
[283] Mallia R J, Subhash N, Mathews A, Kumar R, Thomas S S, Sebastian P and Madhavan J 2010 Clinical grading of oral mucosa by curve-fitting of corrected autofluorescence using diffuse reflectance spectra *Head Neck* **32** 763–79
[284] Mallia R J, Narayanan S, Madhavan J, Sebastian P, Kumar R, Mathews A, Thomas G and Radhakrishnan J 2010 Diffuse reflectance spectroscopy: an alternative to autofluorescence spectroscopy in tongue cancer detection *Appl. Spectrosc.* **64** 409–18
[285] Lin W-C, Mahadevan-Jansen A, Johnson M D, Weil R J and Toms S A 2005 *In vivo* optical spectroscopy detects radiation damage in brain tissue *Neurosurgery* **57** 518–25
[286] De Veld D C G, Skurichina M, Witjes M J H, Duin R P W, Sterenborg H J C M and Roodenburg J L N 2005 Autofluorescence and diffuse reflectance spectroscopy for oral oncology *Lasers Surg. Med.* **36** 356–64
[287] Fabila D *et al* 2012 *In vivo* assessment of liver fibrosis using diffuse reflectance and fluorescence spectroscopy: a proof of concept *Photodiagnosis Photodyn. Ther.* **9** 376–82
[288] Bhatia S, Ragheb J, Johnson M, Oh S, Sandberg D I and Lin W-C 2008 The role of optical spectroscopy in epilepsy surgery in children *Neurosurg. Focus* **25** E24
[289] Majumder S K, Gebhart S, Thompson R, Weaver K D, Johnson M D, Lin W-C and Mahadevan-Jansen A 2007 In-vivo optical detection of brain tumor and tumor margin: a combined auto-fluorescence and diffuse reflectance spectroscopic study *Proc. SPIE* **6430** 64300F

[290] Tanis E, Evers D J, Spliethoff J W, Pully V V, Kuhlmann K, van Coevorden F, Hendriks B H W, Sanders J, Prevoo W and Ruers T J M 2016 *In vivo* tumor identification of colorectal liver metastases with diffuse reflectance and fluorescence spectroscopy *Lasers Surg. Med.* **48** 820–7
[291] Ti Y, Chen P and Lin W-C 2010 *In vivo* characterization of myocardial infarction using fluorescence and diffuse reflectance spectroscopy *J. Biomed. Opt.* **15** 037009
[292] Šćepanović O R, Volynskaya Z, Kong C-R, Galindo L H, Dasari R R and Feld M S 2009 A multimodal spectroscopy system for real-time disease diagnosis *Rev. Sci. Instrum.* **80** 043103
[293] Lin D *et al* 2018 Autofluorescence and white light imaging-guided endoscopic Raman and diffuse reflectance spectroscopy for *in vivo* nasopharyngeal cancer detection *J. Biophoton.* **11** 1–9
[294] Jermyn M, Mercier J, Aubertin K, Desroches J, Urmey K, Karamchandiani J, Marple E, Guiot M C, Leblond F and Petrecca K 2017 Highly accurate detection of cancer in situ with intraoperative, label-free, multimodal optical spectroscopy *Cancer Res.* **77** 3942–50
[295] Jeong S *et al* 2015 Fluorescence-Raman dual modal endoscopic system for multiplexed molecular diagnostics *Sci. Rep.* **5** 9455
[296] Majumder S K, Krishna H, Sidramesh M, Chaturvedi P and Gupta P K 2010 A comparative evaluation of Raman and fluorescence spectroscopy for optical diagnosis of oral neoplasia *Proc. SPIE* **8173** 817306
[297] Badizadegan K *et al* 2004 Spectroscopic diagnosis and imaging of invisible pre-cancer *Faraday Discuss.* **126** 265
[298] Georgakoudi I, Sheets E E, Müller M G, Backman V, Crum C P, Badizadegan K, Dasari R R and Feld M S 2002 Trimodal spectroscopy for the detection and characterization of cervical precancers *in vivo Am. J. Obstet. Gynecol.* **186** 374–82
[299] Georgakoudi I *et al* 2001 Fluorescence, reflectance, and light-scattering spectroscopy for evaluating dysplasia in patients with Barrett's esophagus *Gastroenterology* **120** 1620–9
[300] Langhout G C, Kuhlmann K F D, Schreuder P, Bydlon T, Smeele L E, van Den Brekel M W M, Sterenborg H J C M, Hendriks B H W and Ruers T J M 2018 *In vivo* nerve identification in head and neck surgery using diffuse reflectance spectroscopy *Laryngoscope Investig. Otolaryngol.* **3** 349–55
[301] Kandurova K, Dremin V, Zherebtsov E, Potapova E, Alyanov A, Mamoshin A, Ivanov Y, Borsukov A and Dunaev A 2019 Fiber-optic system for intraoperative study of abdominal organs during minimally invasive surgical interventions *Appl. Sci.* **9** 217
[302] Kandurova K, Dremin V, Zherebtsov E, Potapova E, Filina M, Dunaev A, Mamoshin A, Alyanov A and Muradyan V 2019 Optical diagnostics of bile duct tissues state with tumor compression *Proc. SPIE* **11065** 1106508
[303] Haj-Hosseini N, Richter J C O, Milos P, Hallbeck M and Wårdell K 2018 5-ALA fluorescence and laser Doppler flowmetry for guidance in a stereotactic brain tumor biopsy *Biomed. Opt. Express* **9** 2284
[304] Guided Therapeutics Inc 2014 LuViva® Advanced Cervical Scan_INTL—Early Detection, Better Outcomes® http://myluviva.com/intl/ (Accessed: 17 June 2020)
[305] Safaeian M, Solomon D and Castle P E 2007 Cervical cancer prevention—cervical screening: science in evolution *Obstet. Gynecol. Clin. North Am.* **34** 739–60
[306] Cerussi A, Siavoshi S, Durkin A, Chen C, Tanamai W, Hsiang D and Tromberg B J 2009 Effect of contact force on breast tissue optical property measurements using a broadband diffuse optical spectroscopy handheld probe *Appl. Opt.* **48** 4270–7
[307] Wilson B C, Jermyn M and Leblond F 2018 Challenges and opportunities in clinical translation of biomedical optical spectroscopy and imaging *J. Biomed. Opt.* **23** 030901
[308] Shinozaki S, Miura Y, Ino Y, Shinozaki K, Lefor A K and Yamamoto H 2015 An ultrathin endoscope with a 2.4-mm working channel shortens the esophagogastroduodenoscopy time by shortening the suction time *Clin. Endosc.* **48** 516–21
[309] Stolov A A, Slyman B E, Burgess D T, Hokansson A S, Li J and Allen R S 2013 Effects of sterilization methods on key properties of specialty optical fibers used in medical devices *Proc. SPIE* **8576** 857606
[310] Balog J *et al* 2013 Intraoperative tissue identification using rapid evaporative ionization mass spectrometry *Sci. Transl. Med.* **5** 194ra93
[311] Zhang S *et al* 2019 High- Q polymer microcavities integrated on a multicore fiber facet for vapor sensing *Adv. Opt. Mater.* **7** 1900602
[312] Dietrich P I *et al* 2018 In situ 3D nanoprinting of free-form coupling elements for hybrid photonic integration *Nat. Photonics* **12** 241–7
[313] Power M, Thompson A J, Anastasova S and Yang G Z 2018 A monolithic force-sensitive 3D microgripper fabricated on the tip of an optical fiber using 2-photon polymerization *Small* **14** 1–10
[314] Gissibl T, Thiele S, Herkommer A and Giessen H 2016 Sub-micrometre accurate free-form optics by three-dimensional printing on single-mode fibres *Nat. Commun.* **7** 11763
[315] Thompson A J, Power M and Yang G-Z 2018 Micro-scale fiber-optic force sensor fabricated using direct laser writing and calibrated using machine learning *Opt. Express* **26** 14186
[316] Cui Y, Hegde R S, Phang I Y, Lee H K and Ling X Y 2014 Encoding molecular information in plasmonic nanostructures for anti-counterfeiting applications *Nanoscale* **6** 282–8
[317] Lettrichova I, Pudis D, Gaso P, Jandura D, Kovac Jr J, Laurencikova A, Novak J and Goraus M 2018 Polymer-based 3D microcones for application in SERS *Proc. SPIE* **10976** 109760V
[318] Kim J A, Wales D J, Thompson A J and Yang G-Z 2019 Towards development of fibre-optic surface enhanced Raman spectroscopy probes using 2-photon polymerisation for rapid detection of bacteria *Proc. SPIE* **10894** 10894F
[319] Kim J A, Wales D J, Thompson A J and Yang G-Z 2020 Fiber-optic SERS probes fabricated using two-photon polymerization for rapid detection of bacteria *Adv. Opt. Mater.* **8** 1901934
[320] Kelly C J, Karthikesalingam A, Suleyman M, Corrado G and King D 2019 Key challenges for delivering clinical impact with artificial intelligence *BMC Med.* **17** 195
[321] Hammoudeh S, Gadelhaq W and Janahi I 2018 Prospective cohort studies in medical research *Cohort Studies in Health Sciences*, ed R M Barria (Rijeka: InTech) http://doi.org/10.5772/intechopen.76514
[322] Collins G S, Reitsma J B, Altman D G and Moons K G M 2015 Transparent reporting of a multivariable prediction model for individual prognosis or diagnosis (TRIPOD) the TRIPOD statement *Circulation* **131** 211–9
[323] Collins G S and Moons K G M 2019 Reporting of artificial intelligence prediction models *Lancet* **393** 1577–9
[324] Tonutti M, Elson D S, Yang G Z, Darzi A W and Sodergren M H 2017 The role of technology in minimally invasive surgery: state of the art, recent developments and future directions *Postgrad. Med. J.* **93** 159–67
[325] Gorpas D *et al* 2019 Autofluorescence lifetime augmented reality as a means for real-time robotic surgery guidance in human patients *Sci. Rep.* **9** 1187
[326] Correia R, James S, Lee S-W, Morgan S P and Korposh S 2018 Biomedical application of optical fibre sensors *J. Opt.* **20** 073003

[327] Waterhouse D J, Fitzpatrick C R M, Pogue B W, O'Connor J P B and Bohndiek S E 2019 A roadmap for the clinical implementation of optical-imaging biomarkers *Nat. Biomed. Eng.* **3** 339–53
[328] Leong S, Shaipanich T, Lam S and Yasufuku K 2013 Diagnostic bronchoscopy–current and future perspectives *J. Thorac. Dis.* **5** S498–510
[329] Yang G-Z *et al* 2018 The grand challenges of science robotics *Sci. Robot.* **3** eaar7650
[330] Singh R 2017 Biophotonics Market by End User and Application—Global Opportunity Analysis and Industry Forecast, 2014–2022 https://alliedmarketresearch.com/biophotonics-market (Accessed: 17 June 2020)